Upper Mississippi River Comprehensive Plan For Systemic Flood Damage Reduction and Associated Environmental Sustainability

Draft

Hydrology & Hydraulics

SUPPILMENT TO APPENDIX B

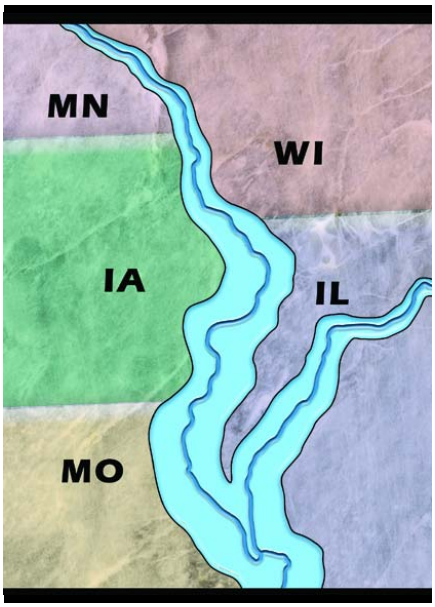

Prepared for the
U.S. Army Corps of Engineers
Rock Island, St. Louis, and St. Paul Districts
By Dr. Robert Barkau

April 2005

UPPER MISSISSIPPI RIVER COMPREHENSIVE PLAN
Hydrology
Supplement to Appendix B

Table of Contents

TITLE PAGE

1.0 Introduction 1
1.1 Event Statistics 4
2.0 Generation of Event Hydrographs at Thebes 7
2.1 Mississippi River Flood Time Series. 7
2.2 Generation of Annual Maximum Flow Time Series 7
2.3 Generate Event Volume. 11
2.3 Generation of Annual Volume. 13
2.4 Generation of Event from Pattern Hydrograph 17
3.0 Generation of Hydrographs at Keokuk, L&D 24, and St. Louis 22
4.0 Generation of the Record for Illinois River Gages 25
4.1 Coincidence 25
4.2 Generation of the Record at Valley City, Kingston Mines, Marseilles, and Lockport. 25
5.0 Generation of the Record at Clinton 31
5.1 The Origin of Floods 31
5.2 Statistics of Generated Hydrographs 32
6.0 Generation of the Record at McGregor, Winona, St. Paul, and Anoka 41
6.1 FFS and Observed Data 41
6.2 Generated Data at McGregor, Winona, St. Paul, and Anoka 42
7.0 Ungaged Inflow 46
8.0 Conclusions and Recommendations. 47

UPPER MISSISSIPPI RIVER COMPREHENSIVE PLAN
Hydrology
Supplement to Appendix B

1.0 Introduction

The most serious problem that has plagued period of record analysis is the shortness of the period of record. For flood analysis, the length of the period of record is seldom long enough to define the high end of the flow frequency curve. For example, the period of flow record for the Mississippi River has only about 63 years of usable record, limited by the length of the tributary gage records. Conventional frequency analysis shows that 1993 flood is about 500-year event at Hannibal and about a 100-year event at Thebes -- a high outlier that plots unrealistically above the scatter of a Weibull Plot. Figure 1 shows a Weibull plot of the Mississippi River at St. Louis. The 1993 flood is above scatter -- about a 200-year event according to the fitted Log-Pearson III distribution.

Secondly, for levee and reservoir analysis, the volume of the event is as important as the maximum flow. For example, after a levee fails, the volume of the flood determines the total impact of the failure. The river stage falls when the levee fails and rebounds after the levee fills. Figure 2 shows the impact of the failure of the McGee Creek levee on stage at Meredosia during the 1979 flood. The stage drops as the storage of the levee fills; afterward the stage rebounds. If the volume of the flood was smaller, the filling of the levee storage would have decapitated the flood crest; instead, only the flux of water through the breach impacted the crest.

If the period of record is long enough, one can assume that every distribution of rainfall is contained within the flood record. For example, at St. Louis, floods originate from the Missouri River, from the upper Mississippi River, from both rivers, from snowmelt in the upper Mississippi and in the upper Missouri basin, and from heavy local rainfall over Missouri and Illinois.

Why not use these floods as patterns, increasing or decreasing the ordinates to create a different maximum flow and stretching or compressing the time step to create a different volume? One burst of rain separates a smaller flood from a larger flood and the reverse. By increasing ordinates and stretching the duration of the flood we are supplying that burst of rain.

In February 1985 the St. Louis gage read 37', 7' above flood stage, and rising. The Quantitative Precipitation Forecast showed a 3" band encircling Central Missouri and Central Illinois. The local Mississippi Tributaries (primarily the Illinois), just upstream of St. Louis, were approaching record stages and were going to receive more rain still. Three inches of rainfall would drive the Mississippi to record stages, breaking the record stage of 43' in 1973. But unexpectedly, the cold front dropped southward and the low-pressure system tracked along the Ohio River, bringing heavy rains and flooding

to Kentucky and Northern Tennessee. One burst of rainfall separated a minor ten-year flood from becoming a record-breaking event.

This work will present 1,000 years of generated record for the Mississippi River from Anoka to Thebes at the mainstem and tributary gages. The algorithm applies the concept of enlarging or reducing the pattern event. For each year the algorithm generated a maximum flow and the volume associated with the maximum flow. A pattern event was selected and an annual volume was generated. The generated time series was compared to the statistics of the observed time series. The quality of the generated sequence was verified by the reproduction of the statistics of the observed time series.

The algorithm extends the period of record, adding rare maximum flow and volumetric events. The generated time series verified by reproducing the observed statistics; we are not changing the statistics, but only increasing the number of events that produced the observed statistics. Alternate time series can be generated at the extreme confidence limits; although, at a cost of about three man months of work. Frequency curves generated from the alternate time series can establish confidence limits on the statistics from the generated period of record.

Presented herein is an algorithm that stochastically generates three statistics:

1) Maximum annual flow.

2) The event volume coincident with the maximum annual flow.

3) The annual volume.

We select annual pattern events from the period of record to generate the annual flow hydrographs.

The algorithm will be proven by generating 1000 years of record along the Mississippi River from Anoka to Thebes and along the Illinois River from Lockport to Valley City. Along the way we will encounter the secondary problems of independence (non-coincident events) along the Illinois River and a transition between snowmelt and rainfall floods between Clinton and Thebes.

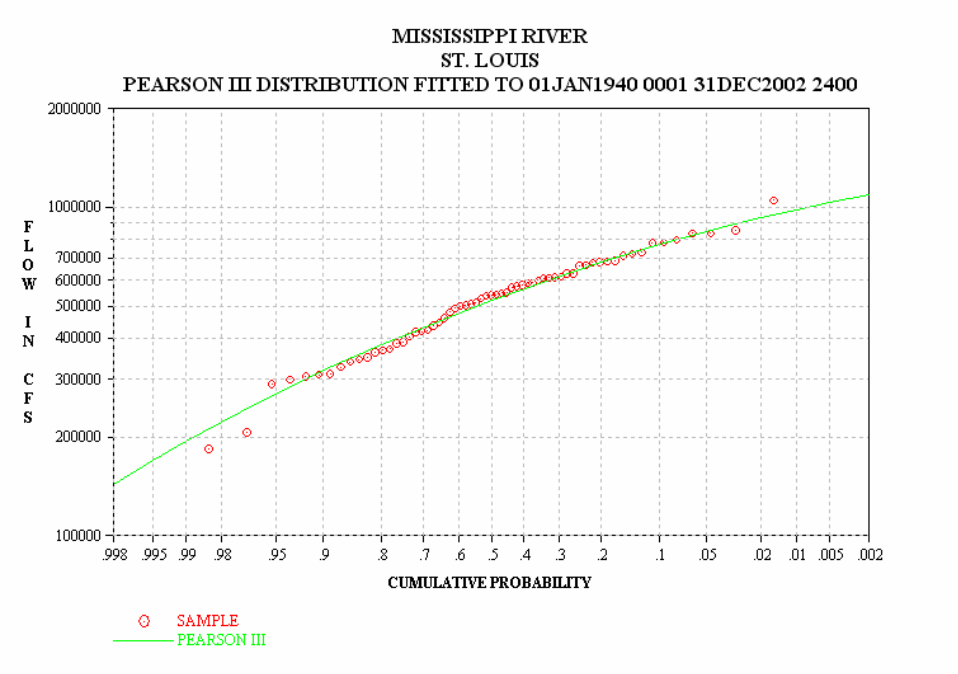

Figure 1. Weibull plot of 63 years of observed maximum flow data at St. Louis. The 1993 flood is a high outlier, plotting above fitted Log-Pearson III frequency curve.

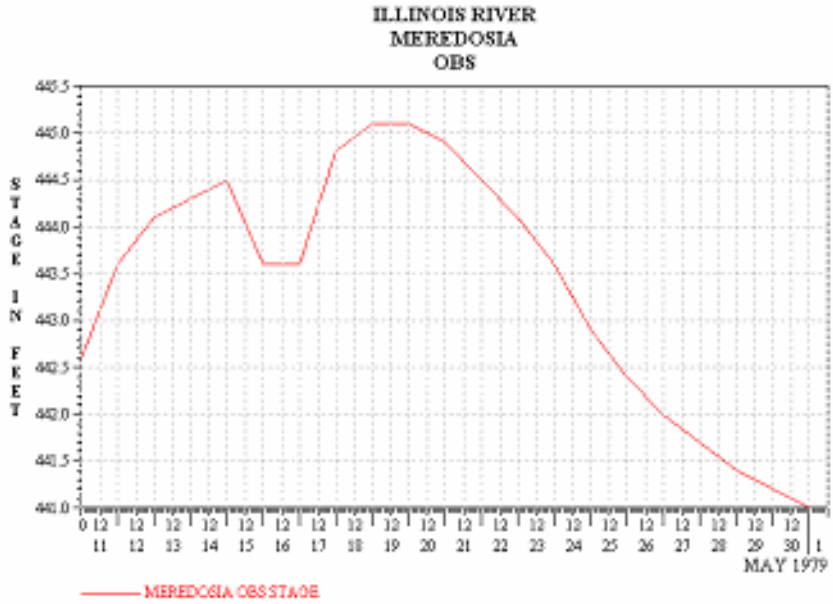

Figure 2. Failure of the McGee Creek levee near the Meredosia gage along the Illinois River. The failure of the levee causes a drop in the water surface until the levee fills when the stage rebounds.

1.1 Event Statistics

The floods are described by the following statistics:

1. The annual maximum flow. Figure 1 shows the Weibull plot of the annual maximum flows from 1940 through 2002.

2. The relationship between maximum flow and the event volume. Figure 3 shows the relationship between maximum flow and event volume at St. Louis. The random scatter demonstrates the wide range of volumes that is associated with any maximum discharge.

3. The volume of the annual maximum flow event. Figure 4 shows the Weibull plot of the volumes associated with the annual maximum flow events at St. Louis.

4. The total annual volume. Figure 5 shows the relationship between the event volume and the total annual volume at St. Louis.

5. The annual duration. Figure 6 shows the annual volume at St. Louis.

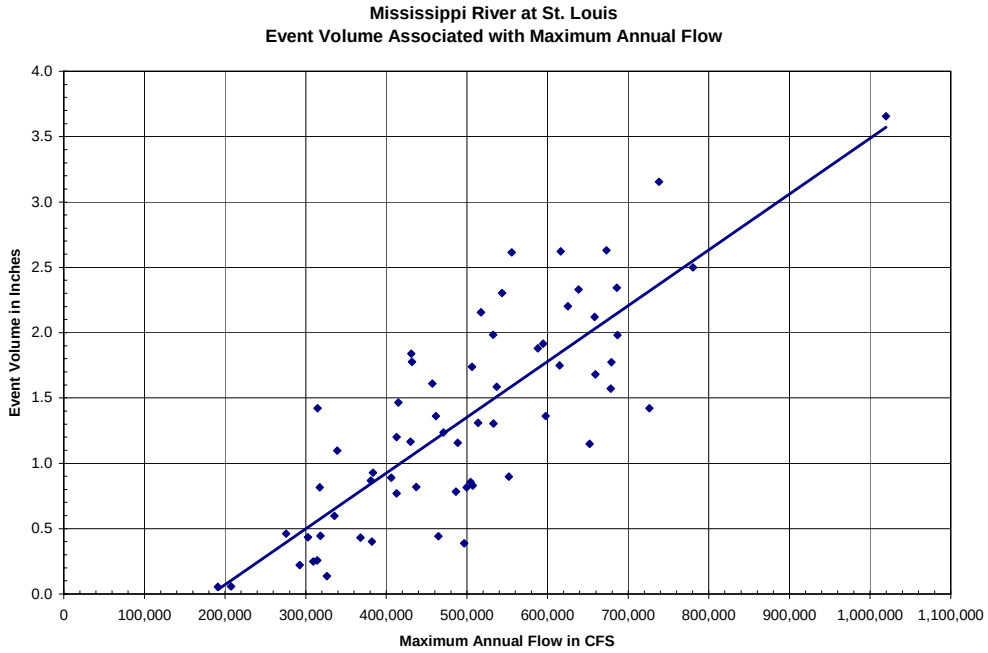

Figure 3. Event volume associated with annual maximum flow from 1940 to 2002 at St. Louis.

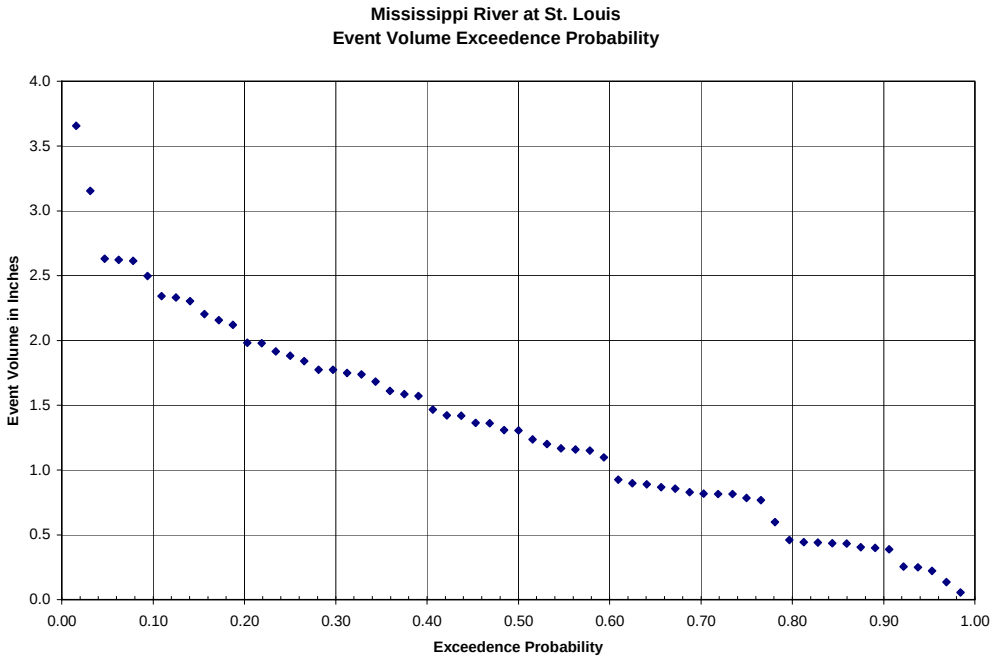

Figure 4. Event volume exceedence probability at St. Louis from 1940 to 2002.

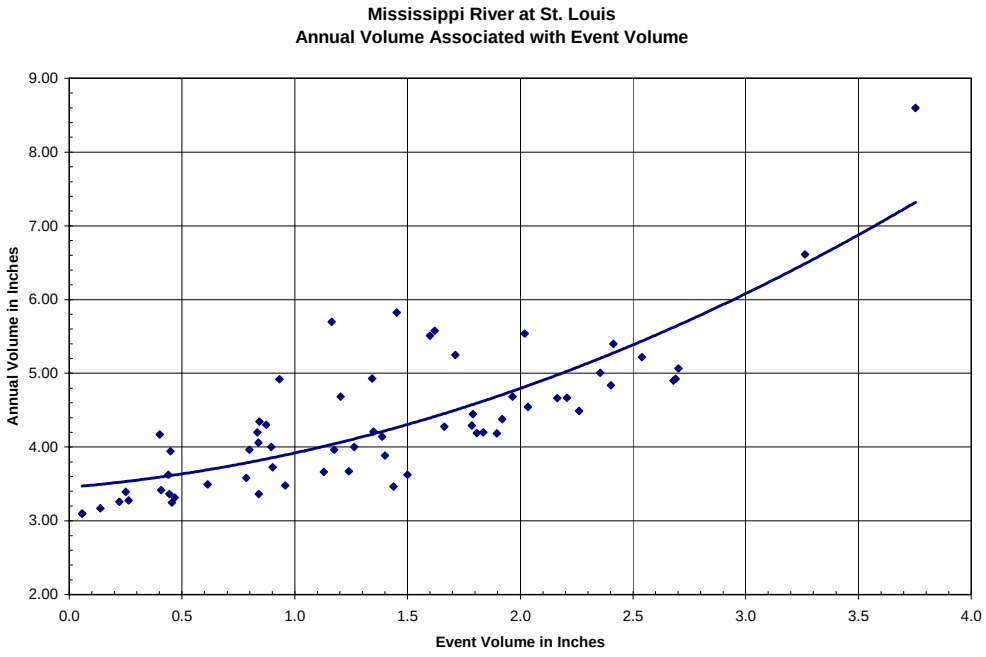

Figure 5. Annual volume associated with event volume at St. Louis from 1940 to 2002.

The start and end, the duration, of a flood is judgmental. Does the flood start and end with median flow? Does it start and end with average annual flow? Almost all Mississippi River floods have multiple crests. Does a flood consist of one crest?

Mississippi River floods result from snowmelt and rainfall. The snowmelt flood occurs in the Spring and may be intensified by rainfall. The rainfall flood can occur any time of year. The author defines a flood beginning with the first rising ordinate below average annual flow and ending with the ordinate after the hydrograph falls below average annual flow. This criterion prevents multiple events from coalescing, forming a huge event.

2.0 Generation of Event Hydrographs at Thebes

The procedure generates events at Thebes that reproduce:

- Annual maximum flow.
- Event volume.
- Annual volume.
- Annual duration.

The following are the steps in the process:

1. Generate time series of annual maximum flows.

2. Generate the event volume that is associated with the annual maximum event.

3. Generate the annual volume.

4. Select the pattern year that has a maximum event with a flow and a volume closest to the generated year.

5. Ratio the flow, the event volume, and the annual volume of the pattern year to create the generated year.

2.1 Mississippi River Flood Time Series.

The time series that was used for all the generated data is the regulated time series that was generated from period of record calculations for FFS. Since we are only studying floods and a much more complex model would be required to study floods and droughts, all flow ordinates less than the median flow were replaced by the median flow at each gage;

$$Q_i = \mathrm{Max}(Q_i , Q_{Med}) ,$$

in which Q_i is a flow ordinate and Q_{Med} is the median flow.

2.2 Generation of Annual Maximum Flow Time Series

The autocorrelation function for the logarithms of the annual maximum time series is shown in Figure 2.1. The observed data shows that the one-parameter autoregressive model, AR(1) model, adequately reproduces the observed autocorrelation function. The autocorrelation table is shown in Table 1. The AR(1) model is

$$z_j = \Phi_1 \, z_{j-1} + \varepsilon \sqrt{\frac{n}{n-1}(1-\Phi_1 \, r_1)} \qquad (2.1)$$

where: z_j = normal deviate from the mean for period j.
Φ_1 = first order autoregressive coefficient; for an AR(1) process $\Phi_1 = r_1$.
ε = random normal deviate from the mean.
n = number of ordinates in the observed sample; from 1940 to 2002, n = 63.
r_1 = observed first order (lag of one) autocorrelation coefficient.

Table 2.1. Autocorrelation of Annual Maximum Flow at Thebes.

Lag	Autocorrelation	Autocorrelation of Logarithms	AR(1) Model Autocorrelation of Logarithms
0	1.00	1.00	1.00
1	0.33	0.36	0.36
2	0.11	0.14	0.13
3	0.14	0.12	0.05
4	0.12	0.08	0.02
5	-0.17	-0.17	0.01
6	-0.19	-0.20	0.00
7	-0.10	-0.12	0.00

The time series is generated from the FFS (Flood Frequency Study) annual maximum flow probability function at Thebes for regulated conditions, which is shown in Figure 2.2. This is a tabular probability-discharge function, which cannot be described by the mean, the variance, and the skewness.

The following steps convert a flow using tabular function into a normal deviate, z:

1. Locate the cumulative probability associated with the flow in the tabular function.

2. Convert the probability into a normal standard deviate. The probability for the normal deviate and the probability for the tabular function would be the same. The conversion equation for a normal cumulative probability to a normal standard deviation, according to Chin, is:

For P < .5, (2.2)

$$z = w - \frac{(A_0 + A_1 w + A_2 w^2)}{(B_0 + B_1 * w + B_2 w^2 + B_3 w^3)};$$

else,

$$z = -\frac{(A_0 + A_1 w + A_2 w^2)}{(B_0 + B_1 * w + B_2 w^2 + B_3 w^3)},$$

where: $w = \sqrt{\log\left(\frac{1}{P^2}\right)}$.

P = probability.
A_0 = 2.515517.
A_1 = 0.802853.
A_2 = 0.010328.
B_0 = 1.000000.
B_1 = 1.432788.
B_2 = 0.189269.
B_3 = 0.001308.

To solve equation 2.1 for the next years flow in the generated sequence, use the following steps:

1. Initiate the time series with a uniformly distributed random number from Microsoft Excel's uniform random number generator, Rnd(). Convert the probability into flow using the tabular function. Convert the maximum flow into a normal standard deviate, z_1.

2. Use the normal standard deviate, z_{j-1}, from the previous year.

3. Generate a random standard deviate, ε. Generate a uniformly distributed probability using Rnd(). Convert the uniform probability into the normal random standard deviate, ε, using equation 2.2.

4. Solve equation 2.1 for the next normal deviation, z_j, in the generated sequence.

5. Iteratively solve equation 2.2 for the probability, P_j, associated with the normal deviation, z_j.

6. Find the flow from the tabular function that is associated with P_j from step 5.

7. Continue with step 2.

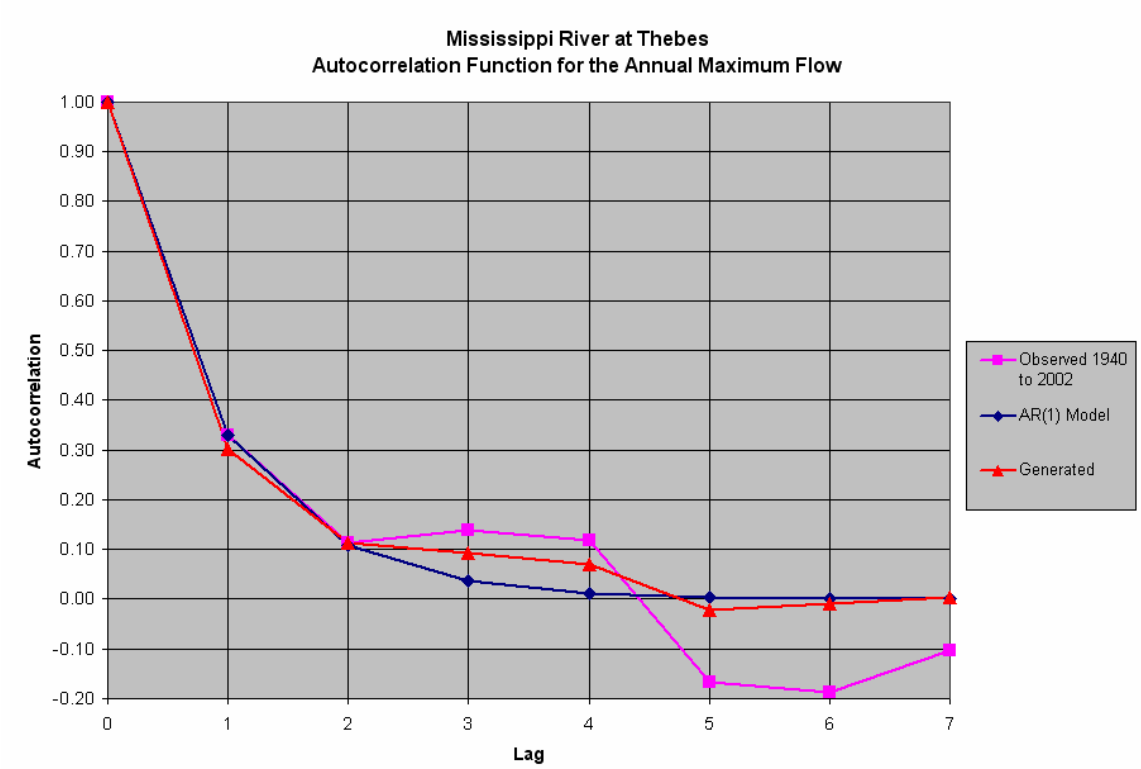

Figure 2.1. Autocorrelation function for the logarithms of annual maximum flow at Thebes. The observed data is adequately represented by the AR(1) model.

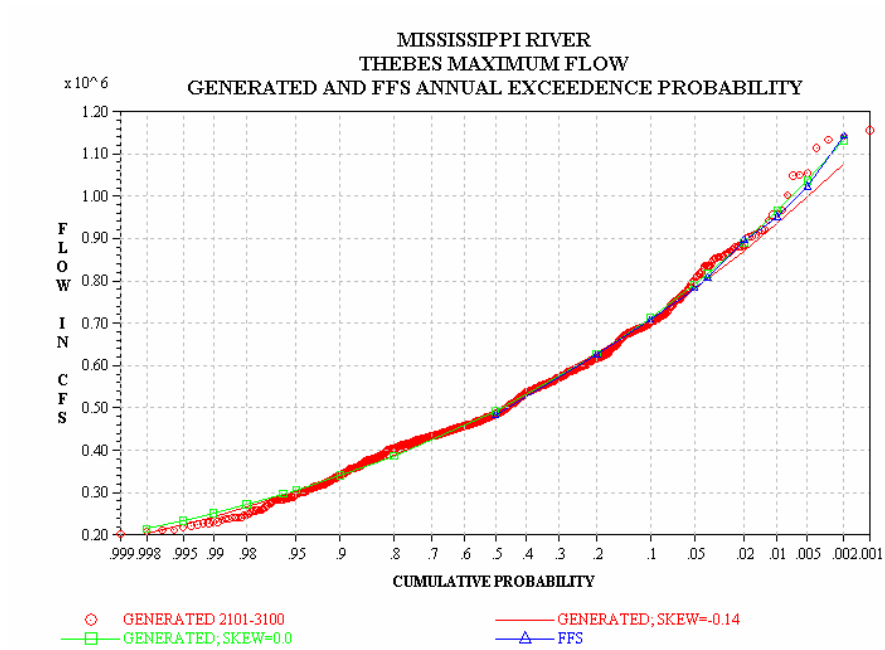

Figure 2.2. The blue line is FFS annual maximum probability function at Thebes. The red circles area Weibull plot of the generated record. The green line is a Pearson III distribution fitted to the generated record with the adopted regional skew of 0.0.

Figure 2.2 compares the statistics of the generated record compared to the FFS probability function. The generated record reproduces the FFS distribution. The generated autocorrelation function is shown on Figure 2.1.

2.3 Generate Event Volume.

The event volume is the volume in inches of runoff of the annual maximum event. The time period of an event extends from the crest backward to average annual flow and forward from the crest to average annual flow.

We investigate the relationship between maximum discharge and event volume. The observed time series is divided into flow regions: Over 750,000 CFS; 550 to 750,000 CFS; 350 to 550,000 CFS; and under 350,000 CFS. Figure 2.3 shows discharge plotted against event volume for the regions. One can see an overall correlation between maximum discharge and event volume ($r^2 = 0.68$), but one also can see a large amount of scatter. For example, the observed range of event volume for 750,000 CFS is from 1.4 to 3.3 inches. Table 2.2 summarizes the statistics for the flow regions. We see that the linear regression of discharge on event volume defines only a small fraction of the variance of event volume. Furthermore, at the 90% confidence level, one can reject the hypothesis that the correlation coefficient is different from zero.

Table 2.2. Statistics of a linear regression of discharge upon event volume.

Region	r^2 Fraction Variance Explained by Discharge	r Correlation Coefficient	Standard Deviation of Residuals Inches
Over 750,000 CFS	0.39	0.62	0.66
550 to 750,000 CFS	0.12	0.34	0.54
350 to 550,000 CFS	0.19	0.44	0.45
Under 350,000 CFS	0.27	0.52	0.22

We assume that event volume is independent of discharge over the flow regions. Hence, for each flow region we rank all the observed event volumes and develop a marginal probability relationship. Figure 2.4 shows the marginal event volume probability functions for the four regions. We do not try to fit a distribution to the Weibull plot; instead, we define the cumulative distribution function with a quadratic equation.

To assign an event volume to a maximum flow, we follow these steps:

1. Generate a uniform random probability using the Rnd() function.

2. For maximum flow $Q_{max\ j}$, locate a region that contains $Q_{max\ j}$.

3. Solve the associated quadratic equation for the event volume, using the probability of step 1.

4. Return to step 1.

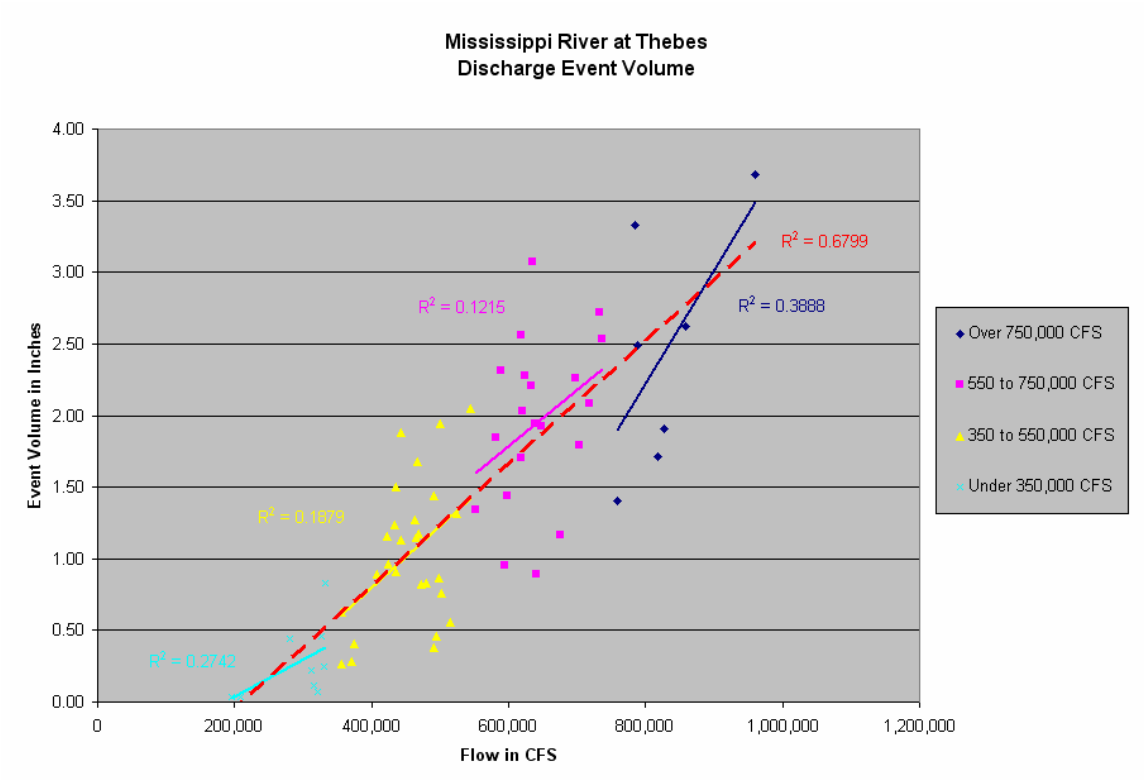

Figure 2.3. Discharge-event volume relationship at Thebes. The dotted red line is fitted to the overall scatter of data. The other lines are fitted to the four flow regions. One sees that the scatter is profound and that the correlation is poor in the flow regions.

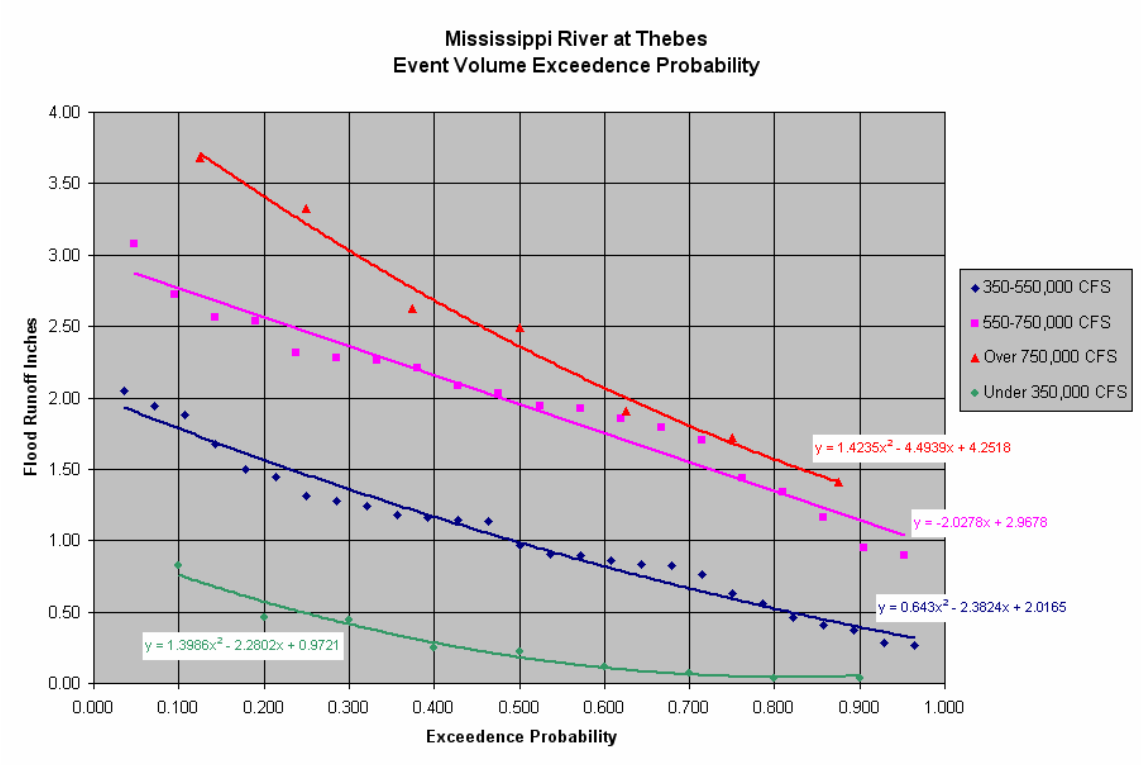

Figure 2.4. Marginal probability density functions for the four flow regions. Quadratic equations were fitted to the Weibull plots.

Figure 2.5 compares the generated event volume cumulative probability and the observed event volume cumulative probability.

2.3 Generation of Annual Volume.

The annual volume is the total volume for the generated year. Annual volume is only used to fill out the residual events for the year. Figure 2.7 shows the relationship between the event volume and average annual volume. A quadratic function is fitted to the curve. From an analysis of the residual, we find that the standard deviation of the residual is 0.56 inches and that the skewness is 1.36 (the distribution of the residuals is skewed toward the higher volume). We assume that the residuals are described by the Pearson III distribution. The mean is the regression line; the standard deviation is 0.56 inches; and the skewness is 1.36. The standard deviation and skewness properties are assumed uniform along the regression line.

The following steps generate annual event volumes:

1. Generate a uniform random probability using the Rnd() function.

2. Calculate the mean annual volume by applying the event volume to the quadratic equation.

3. Using the random probability, the mean, standard deviation, and the skewness, calculate the annual volume from the Pearson III distribution.

4. Return to step 1 for the next year.

Figure 2.8 shows the relationship between generated annual volume and observed annual volume.

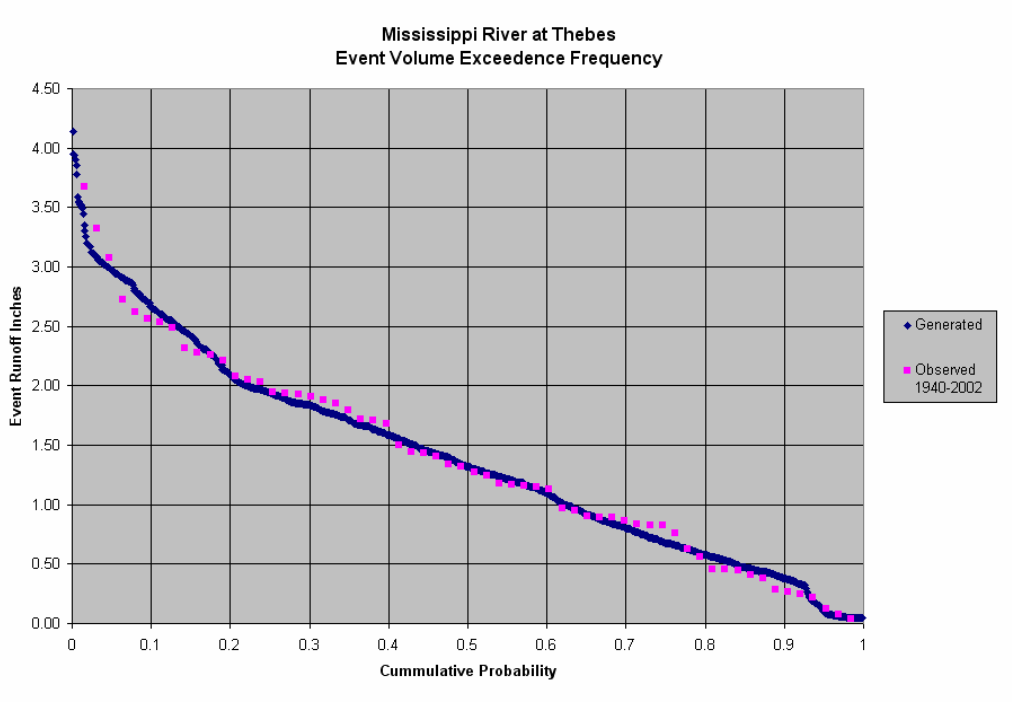

Figure 2.5. Generated and observed event volume exceedence probability at Thebes.

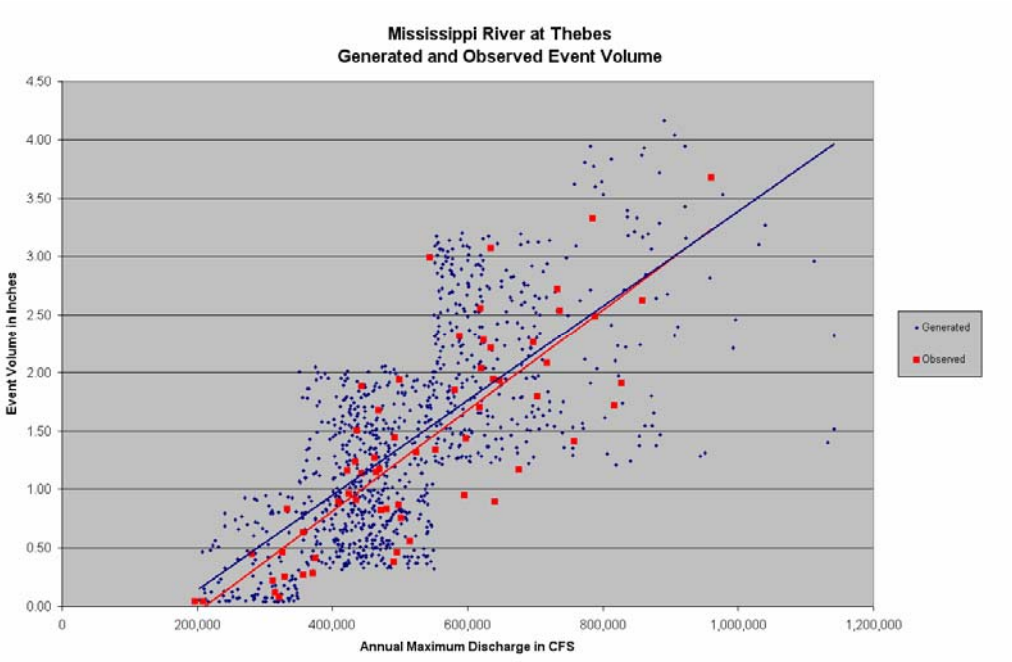

Figure 2.6. Generated and observed event volume at Thebes.

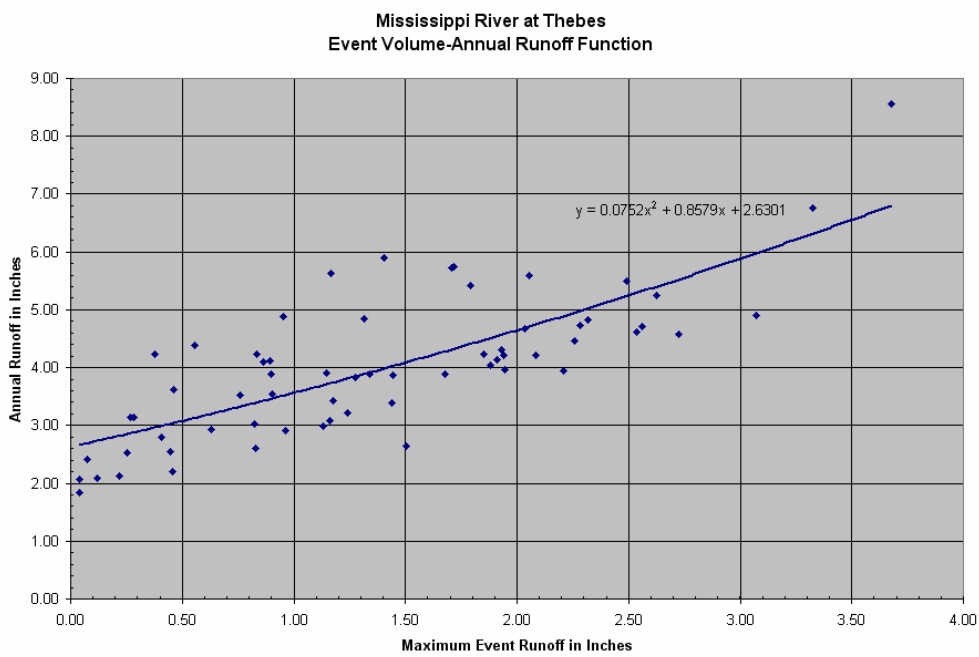

Figure 2.7. Observed event volume-annual volume function at Thebes. The residuals are skewed above the curve.

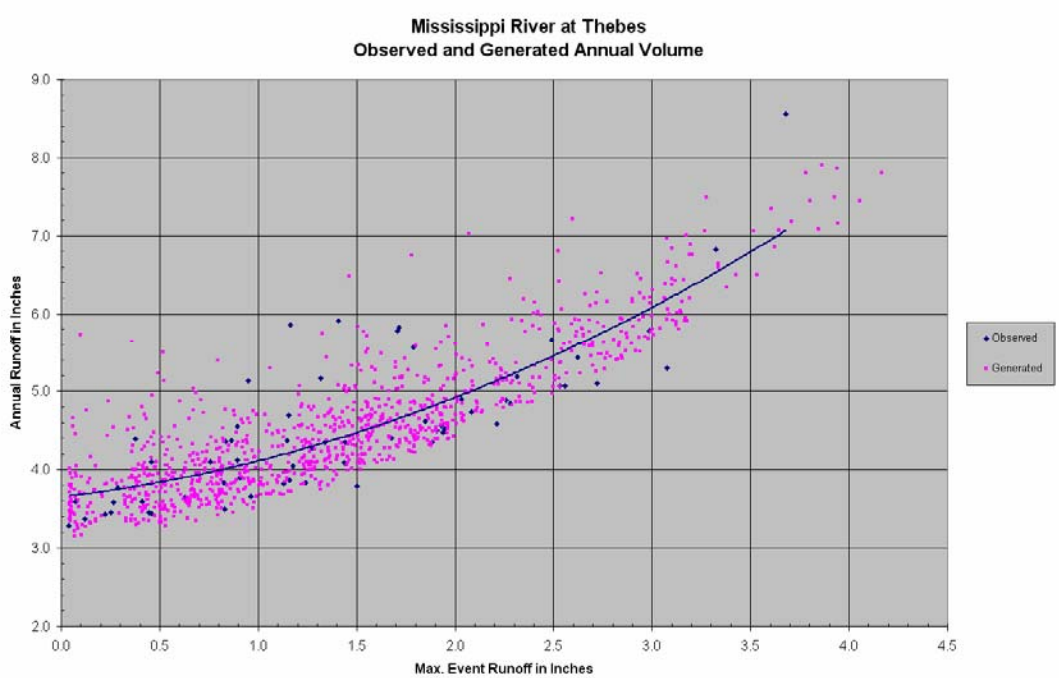

Figure 2.8. Observed and generated annual volume at Thebes. The Pearson III distribution of the residuals reproduces the skew of the observed data.

2.4 Generation of Event from Pattern Hydrograph

Each year of the generated period is patterned after an observed year. The pattern year is chosen such that the observed crest and event volume is close to the generated data, but slightly smaller, so that the observed event is ratioed upward. The hydrographs are generated backwards, from 3100 to 2101.

Also the December 1982 flood extends to 21 January 1983. For this reason, the 1982 flood is lagged backward two months to 1 October and the first 21 days of January 1983 are set to the median flow.

We will use the generation of a hydrograph for the year 2185 as an example. The basic data for 2185 is shown below.

	Annual Maximum Flow CFS	Event Volume Inches	Annual Volume Inches
2185 Generated	866,584	3.19	6.89
1973 Pattern	785,220	3.32	6.82

The following steps generate a hydrograph for the year 2185:

1. Multiply the ordinates of the pattern event, from 3/8/1973 to 6/27/1973, by 1.104. All other ordinates outside of the event are set to the median flow of 172,000 CFS. Figure 2.9 shows the resulting hydrograph.

2. Reduce the time base of the hydrograph to produce an event volume of 3.19 inches. The time interval of the period average ordinates is reduced from 24 hours to 20.74 hours. The interval 20.74 hours was optimized by iteration with a tolerance of .01 inches; hence, the optimized event volume of 3.20 inches. The ordinates of the revised hydrograph are finally converted to an interval of 24 hours. The revised hydrograph is shown in Figure 2.10.

3. Add the residual portion of the hydrograph. The residual portion is the hydrograph outside the event. The residual increases the annual volume to the generated volume. A three-day transition is provided to and from the event and a five-day transition period is from 27 December to 1 January of the next year. **The year-to-year transition is the reason that the hydrographs are generated backwards.** Figure 2.11 shows the hydrograph with the residual.

Figure 2.12 shows a composite of steps one to three.

Figure 2.13 shows a segment of the table that summarizes the statistics of the generated events at Thebes. The events extend from 2101 to 3100.

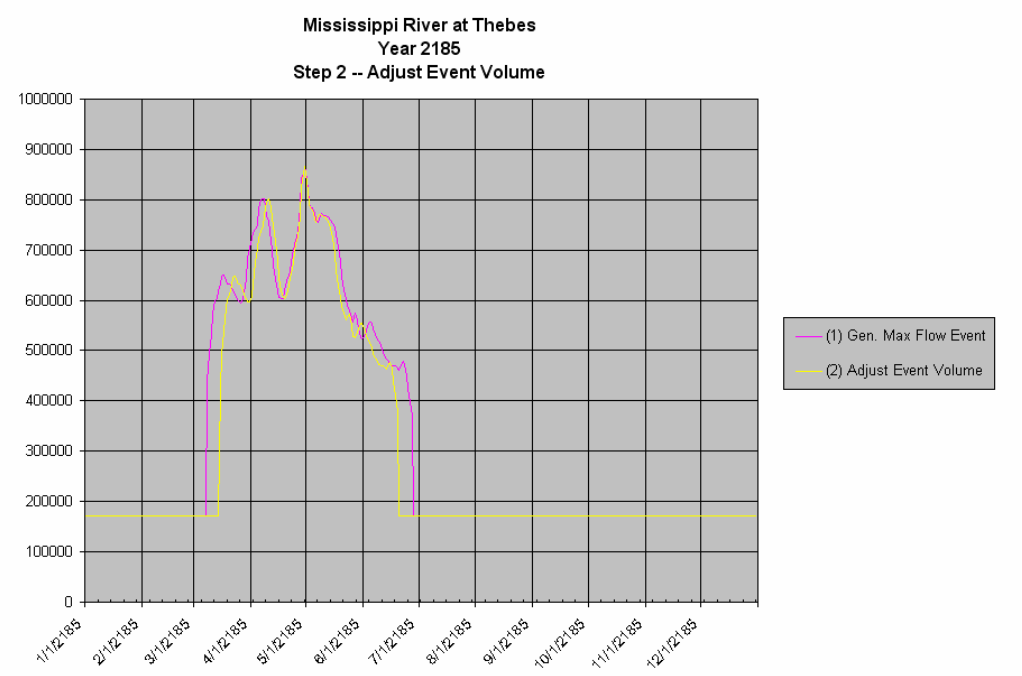

Figure 2.9. Step 1: We multiply the ordinates of maximum event of the pattern year 1973 by 1.104, increasing the 1973 maximum flow to 866,584 CFS. All other ordinates outside the maximum event are set to the median flow of 172,000 CFS.

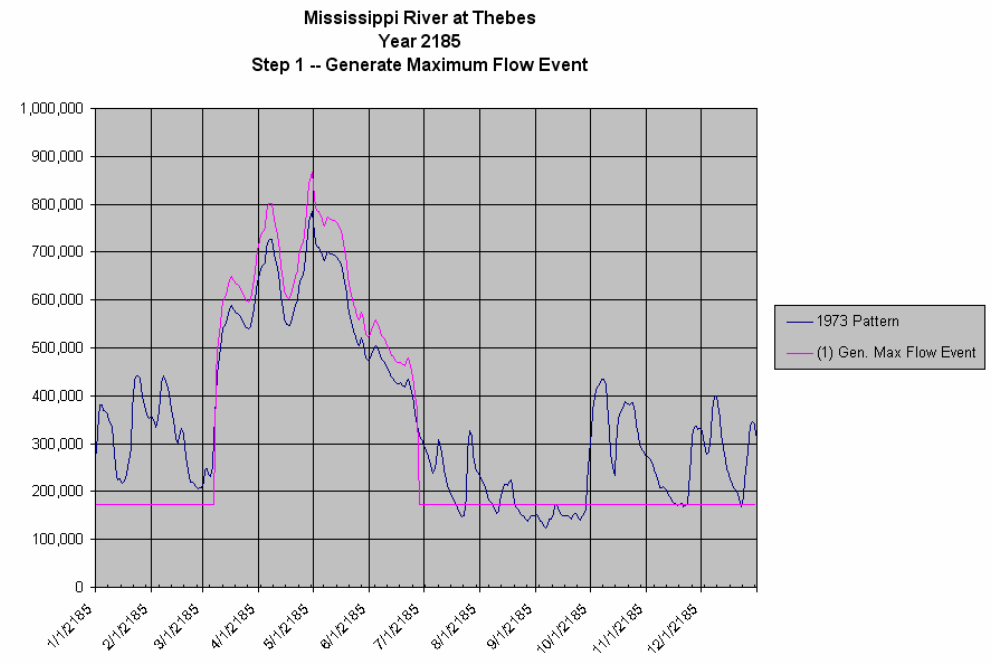

Figure 2.10. Step 2: The time base of the event hydrograph is reduced to reproduce an event volume of 3.19 inches.

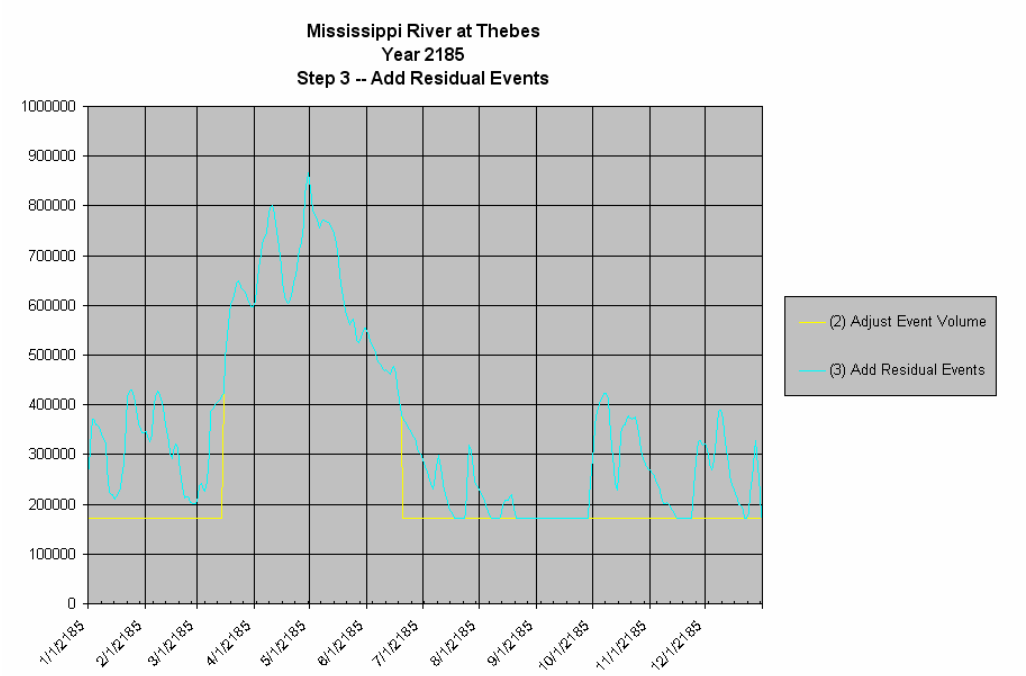

Figure 2.11. Step 3: The residual hydrograph is added before and after the event. The residual hydrograph increases the volume to the generated volume.

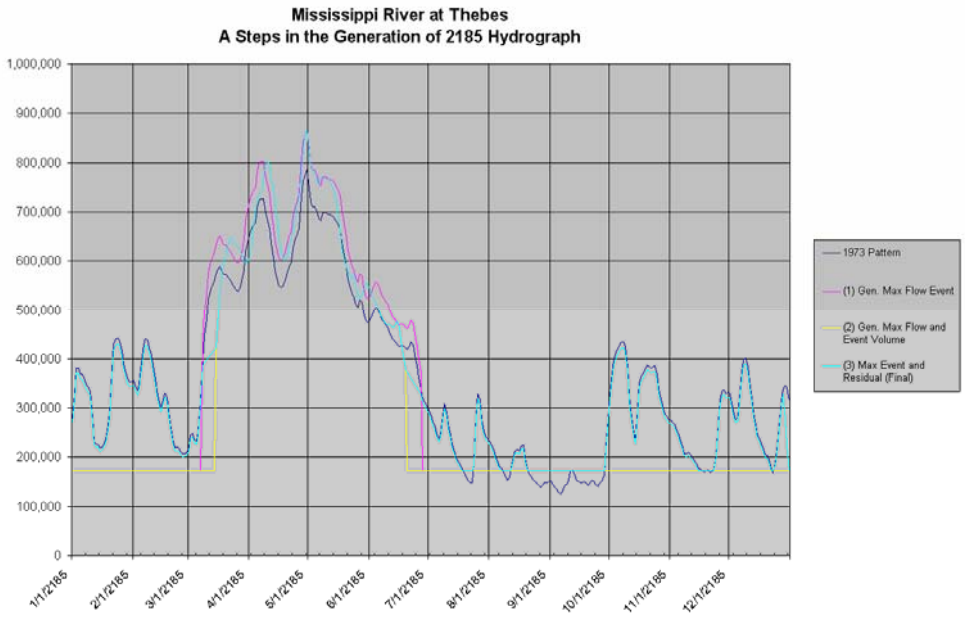

Figure 2.12. All steps. The generated hydrograph is a minor modification from the 1973 pattern event.

Mississippi River at Thebes
Statistics of Generated Events

Year	Generated Statistics			Pattern Hydrograph						Output Hydrograph							
	Max Flow CFS	Volume Inches	Annual Runoff Inches	Max Flow in CFS	Volume in Inches	Year	Starting Date	Ending Date	Max Flow Factor	Max Flow CFS	Event Volume Inches	Time Step Hours	Max Event Starting Date	Max Event Ending Date	Residual Flow Factor	Annual Runoff Inches	Annual Volume Error Inches
2101	572260	1.87	4.53	499,423	1.94	1975	2/20/1975	6/13/1975	1.146	572,260	1.88	20.07	3/2/2101	6/5/2101	0.92	4.54	0.00
2102	581433	1.87	4.88	580,797	1.85	1978	3/14/1978	6/12/1978	1.018	581,433	1.87	23.73	3/14/2102	6/11/2102	1.18	4.88	0.00
2103	380821	1.75	4.54	332,818	0.83	1953	3/16/1953	5/25/1953	1.144	380,821	1.75	44.15	2/26/2103	7/5/2103	2.23	4.54	0.01
2104	343364	0.10	3.33	311,030	0.22	1964	6/10/1964	7/5/1964	1.101	343,364	0.10	16.26	6/21/2104	7/3/2104	-901.00	3.35	-0.02
2105	347894	0.12	3.68	314,919	0.12	1989	9/12/1989	9/21/1989	1.105	347,894	0.12	19.68	9/12/2105	9/19/2105	1.45	3.68	0.01
2106	427987	0.82	3.70	408,511	0.90	1972	4/3/1972	5/30/1972	1.048	427,987	0.82	20.80	4/6/2106	5/25/2106	0.85	3.71	-0.01
2107	479833	1.41	4.86	462,485	1.27	1949	2/12/1949	4/29/1949	1.037	479,833	1.40	25.49	2/10/2107	5/1/2107	1.17	4.86	0.00
2108	444015	0.65	4.17	356,344	0.63	1900	3/20/1900	5/4/1900	1.246	444,015	0.66	19.75	3/22/2108	4/28/2108	1.39	4.17	0.00
2109	628734	1.35	4.01	587,998	1.44	1948	3/1/1948	5/28/1948	1.051	628,734	1.36	21.32	3/3/2109	5/21/2109	0.86	4.02	0.00
2110	673430	1.56	4.37	617,849	1.71	1998	3/10/1998	5/19/1998	1.090	673,430	1.56	19.90	3/16/2110	5/13/2110	0.43	4.39	-0.01
2111	526997	1.46	4.33	491,960	1.44	1970	4/16/1970	7/3/1970	1.071	526,997	1.46	22.40	4/17/2111	6/29/2111	0.93	4.33	0.00
2112	560268	2.18	5.37	499,423	1.94	1975	2/20/1975	6/13/1975	1.122	560,268	2.18	23.68	2/20/2112	6/12/2112	1.38	5.37	0.00
2113	812457	2.41	4.98	789,024	2.49	1983	3/9/1983	8/13/1983	1.030	812,457	2.41	22.38	3/12/2113	8/10/2113	0.84	4.98	0.00
2114	553546	1.40	4.64	552,651	1.34	1962	3/14/1962	5/23/1962	1.002	553,546	1.39	24.74	3/13/2114	5/24/2114	1.10	4.64	0.00
2115	557083	2.70	5.63	544,476	2.99	1984	3/18/1984	7/20/1984	1.023	557,083	2.70	21.09	3/22/2115	7/8/2115	0.95	5.63	0.00
2116	574457	2.43	5.18	544,476	2.99	1984	3/18/1984	7/20/1984	1.055	574,457	2.43	18.34	3/27/2116	8/30/2116	0.70	5.18	0.00
2117	357425	1.16	3.98	332,818	0.83	1953	3/16/1953	5/25/1953	1.074	357,425	1.16	31.03	3/9/2117	6/8/2117	1.53	3.98	0.00
2118	336248	0.07	3.21	314,919	0.12	1989	9/12/1989	9/21/1989	1.068	336,248	0.07	10.37	9/13/2118	9/17/2118	-901.00	3.30	-0.09
2119	444347	0.43	3.87	375,225	0.41	1977	10/27/1977	11/28/1977	1.184	444,347	0.43	20.92	10/28/2119	11/23/2119	1.01	3.87	0.00
2120	393226	0.91	4.05	332,818	0.83	1953	3/16/1953	5/25/1953	1.182	393,226	0.91	22.01	3/17/2120	5/20/2120	1.49	4.05	0.00
										.							
										.							
										.							
2184	355267	0.78	3.74	332,818	0.83	1953	3/16/1953	5/25/1953	1.067	355,267	0.78	20.27	3/19/2184	5/17/2184	1.27	3.74	0.00
2185	866504	3.19	6.09	785,220	3.32	1973	3/8/1973	6/27/1973	1.104	866,504	3.20	20.74	3/15/2185	6/19/2185	0.97	6.09	0.00
2186	400922	1.01	4.23	464,706	1.14	1950	4/24/1950	7/3/1950	1.035	400,922	1.01	20.21	4/27/2186	6/25/2186	0.94	4.23	0.00
										.							
										.							
										.							
3093	541021	1.70	5.37	467,978	1.68	1952	3/11/1952	6/4/1952	1.156	541,021	1.70	20.91	3/12/3093	5/25/3093	1.50	5.37	0.00
3094	601500	2.74	6.52	544,476	2.99	1984	3/18/1984	7/20/1984	1.105	601,500	2.74	19.80	3/25/3094	7/5/3094	1.29	6.52	0.00
3095	591783	1.64	4.57	580,797	1.85	1978	3/14/1978	6/12/1978	1.019	591,783	1.63	20.74	3/16/3095	6/1/3095	1.03	4.58	0.00
3096	508420	0.80	4.10	501,239	0.76	1967	6/11/1967	7/20/1967	1.014	508,420	0.80	24.66	6/10/3096	7/20/3096	0.97	4.10	0.00
3097	513697	0.79	3.50	501,239	0.76	1967	6/11/1967	7/20/1967	1.025	513,697	0.80	24.14	6/10/3097	7/20/3097	-901.00	3.71	-0.20
3098	641985	1.28	4.80	597,998	1.44	1948	3/1/1948	5/28/1948	1.074	641,985	1.28	19.71	3/5/3098	5/16/3098	1.65	4.81	0.00
3099	455945	1.16	4.18	443,031	1.13	1957	5/17/1957	8/5/1957	1.029	455,945	1.16	23.72	5/17/3099	8/4/3099	1.41	4.18	0.00
3100	548832	1.81	4.39	499,423	1.94	1975	2/20/1975	6/13/1975	1.099	548,832	1.81	20.26	3/2/3100	6/5/3100	0.85	4.39	0.00

Figure 2.13. Summary of the generated events at the Thebes gage. A residual flow factor of -901 means that the algorithm could not converge to a residual volume.

3.0 Generation of Hydrographs at Keokuk, L&D 24, and St. Louis

Each annual event generated at Thebes represents an annual time series between Keokuk and Thebes. We assume:

1. The maximum event at Thebes is also the maximum event at Keokuk, L&D 24, and St. Louis.

2. The annual hydrographs between Keokuk and Thebes can be uniformly adjusted by the maximum flow factor, the event boundaries, the adjusted event time step, and residual volume factor.

These assumptions are verified by comparing the generated statistics to the base observed statistics. Figure 3.1 compares the generated Weibul maximum flow frequency plot at St. Louis with the observed and FFS statistics; Figure 3.2 compares the generated Weibul event volume frequency plot and the observed event volume frequency plot; Figure 3.3 compares the generated scatter of annual volume and the scatter of observed annual volume; and Figure 3.4 compares the generated and the observed stage duration plots. The generated data reproduces the observed statistics, verifying the above assumptions. Appendix A shows the generated and observed statistics at Keokuk, L&D 24, St. Louis, and Thebes. The quality of the results verify the algorithm.

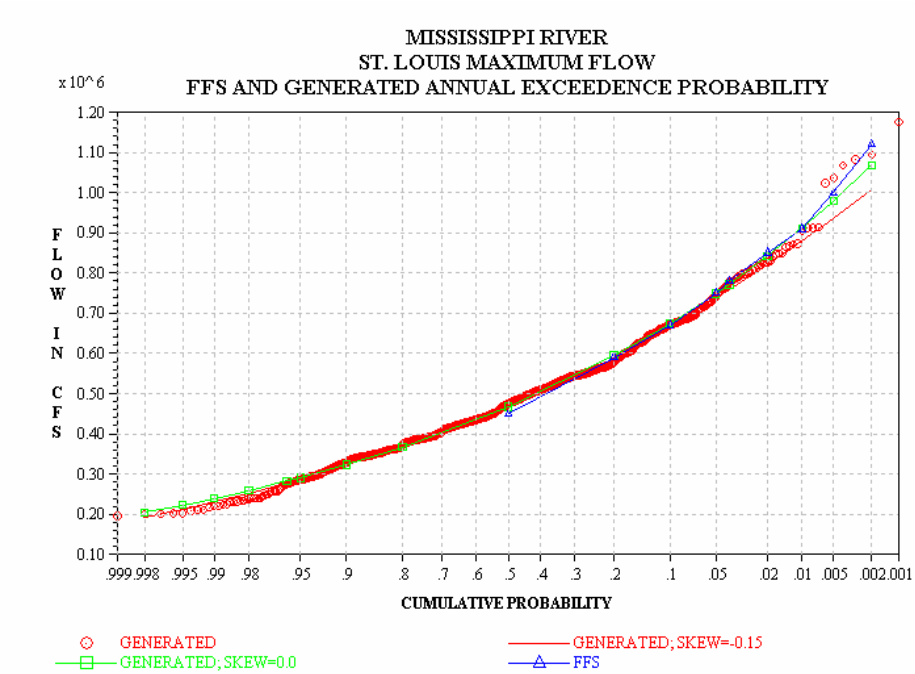

Figure 3-1. Maximum flow exceedence frequency at St. Louis for FFS and for generated data from 2101 to 3100. The actual skew, -0.15, is used for the generated Log-Pearson III curve. FFS applied a regional skew of 0. 00.

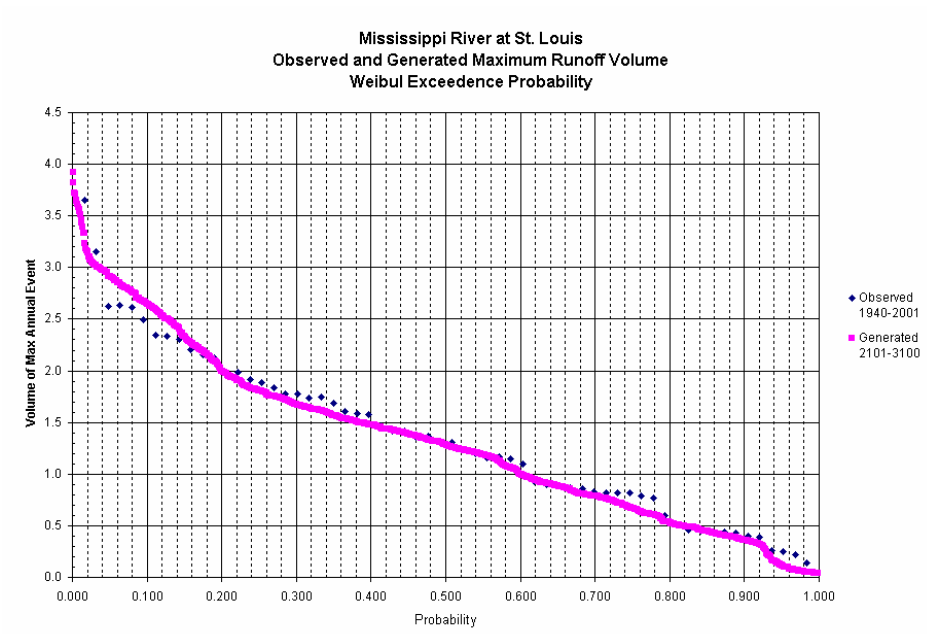

Figure 3-2. Event volume frequency at St. Louis for observed data from 1940 to 2002 and for generated data from 2101 to 3100.

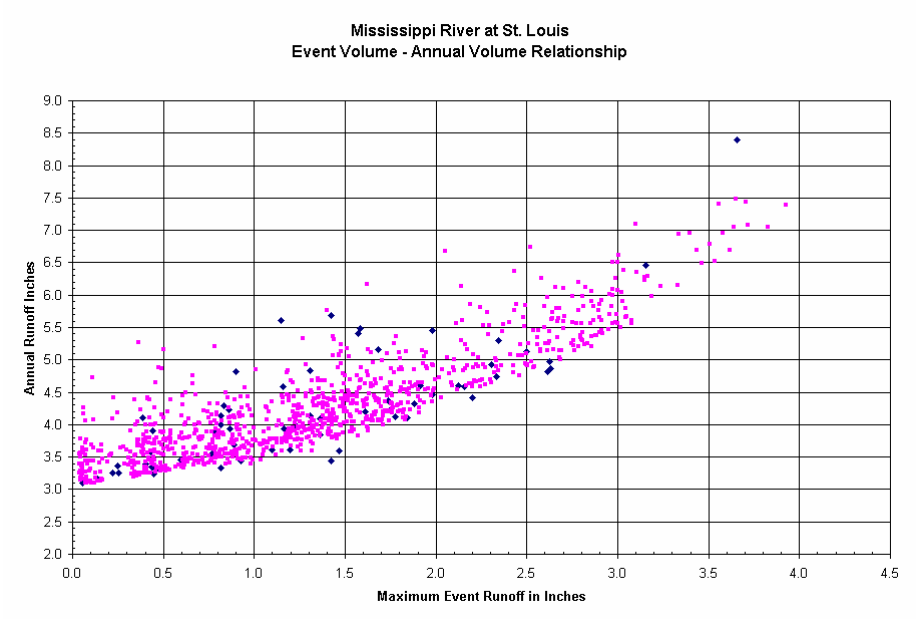

Figure 3-3. Annual volume at St. Louis for observed data from 1940 to 2002 and for generated data from 2101 to 3100.

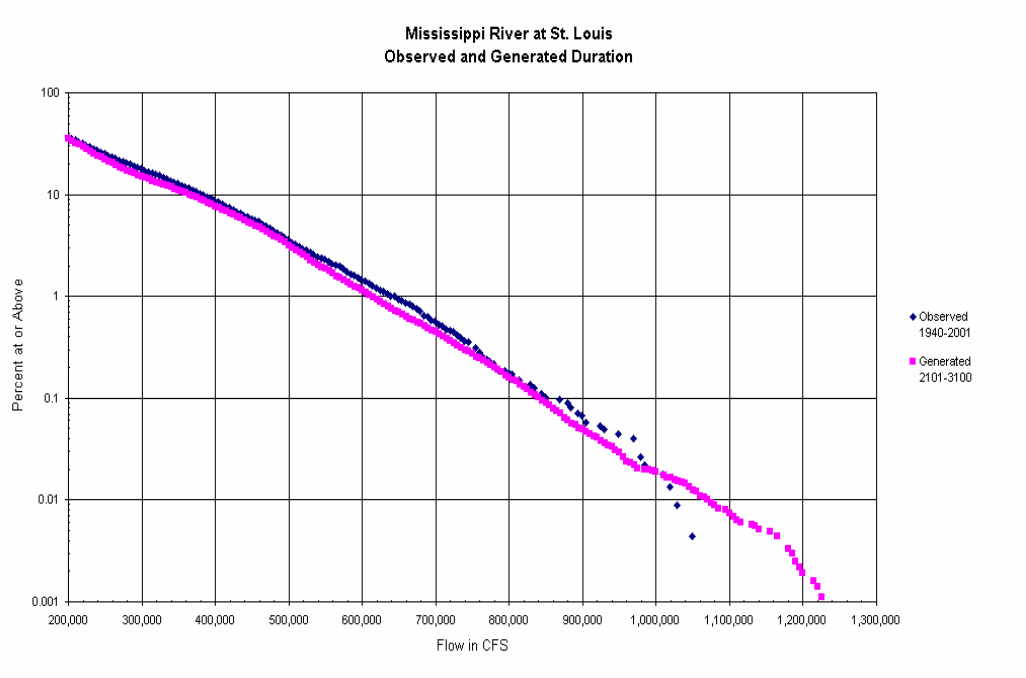

Figure 3-4. Annual duration at St. Louis for observed data from 1940 to 2002 and for generated data from 2101 to 3100.

4.0 Generation of the Record for Illinois River Gages

4.1 Coincidence

Backwater from the Mississippi River is the predominant cause of flooding along the lower Illinois River downstream of La Grange. While backwater may extend up to Kingston Mines, flow increasingly becomes the dominant cause. Sometimes, the headwater crests do not coincide with the Mississippi River events. Table 4.1 lists the Illinois River crests and the Mississippi River crests. Non-coincident events are marked with an "X". Note that the largest events, those with flow greater than 100,000 CFS are always coincident with the Mississippi River. To simulate the shape of the middle of the frequency curve, we must simulate these non-coincident events.

Figure 4.1 shows the relationship between the crest coincident with the Mississippi River and the primary crest. We assume that the scatter is normally distributed about the trend-line. Figure 4.2 shows the relationship between the primary headwater event volume and the secondary Mississippi River event volume.

To generate the non-coincident event, we use the following procedure:

1. Apply the generated Illinois River crest coincident with the Mississippi River to Figure 4.1. The coincident Illinois River crest is the maximum flow times the Mississippi River maximum flow factor.

2. Estimate a deviation off the mean trend-line using a normally distributed random number and the standard deviation of the residuals. The deviation plus the average maximum flow of step 1 gives the crest of the non-coincident event.

3. Apply the non-coincident crest to Figure 4.2 to determine the event volume.

4.2 Generation of the Record at Valley City, Kingston Mines, Marseilles, and Lockport.

Appendix B compares the generated statistics to the FFS frequency curve and the observed statistics. Table 2.2 shows the statistics of the generated events. As a sample, Figures 4.3 to 4.6 compare the frequency curves, the event volume frequency curves, the annual volume relationships, and duration curves. Figures 4.7 shows the flow hydrographs at Lockport, Marseilles, Kingston Mines, and Valley City for the generated year 2108. The major event in June is not coincident with the Mississippi River maximum event; therefore, the non-coincident crest was generated. Figure 4.8 shows the generated hydrographs for 2214. The crest in March was coincident with the Mississippi River crest. The second crest in November was not generated, but instead it was a part of the residual.

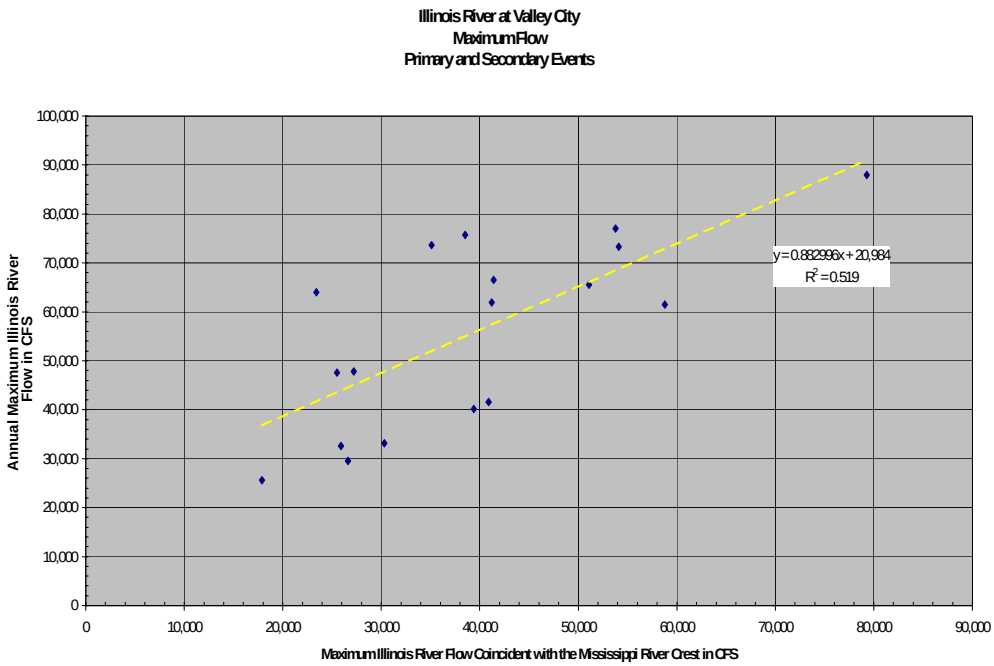

Figure 4.1. Relationship between the Illinois River crest coincident with Mississippi River and with the non-coincident crest.

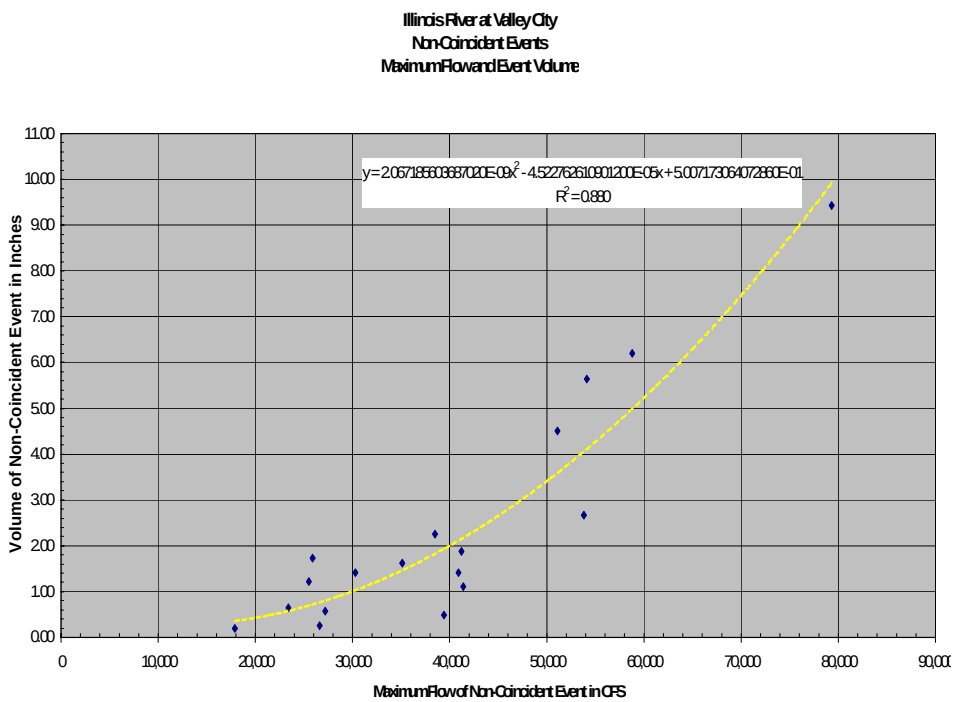

Figure 4.2. Relationship between non-coincident event maximum flow and event volume.

Table 4.1 Coincidence of Illinois River and Mississippi River Crests								
	Valley City					Thebes		
Year	Starting Date	Ending Date	Max Flow CFS	Date Max Flow	Not Coincident	Starting Date	Ending Date	Max Flow CFS
1940	3/3/1940	3/15/1940	25600	03/08/1940	X	6/14/1940	6/18/1940	208607
1941	10/4/1941	12/18/1941	44200	10/17/1941		10/5/1941	12/14/1941	469138
1942	2/4/1942	5/7/1942	73600	02/17/1942	X	6/10/1942	7/24/1942	479712
1943	4/25/1943	7/16/1943	123000	05/27/1943		4/15/1943	7/28/1943	697383
1944	3/13/1944	6/21/1944	101000	04/29/1944		4/11/1944	7/15/1944	717397
1945	4/2/1945	7/13/1945	62700	05/24/1945		3/3/1945	7/14/1945	634477
1946	1/1/1946	2/12/1946	65900	01/14/1946		1/8/1946	1/27/1946	491032
1947	3/24/1947	7/20/1947	67600	06/12/1947		4/4/1947	7/22/1947	732234
1948	2/21/1948	5/3/1948	73500	04/01/1948		3/1/1948	5/28/1948	597998
1949	1/17/1949	4/30/1949	58000	02/27/1949		2/12/1949	4/29/1949	462465
1950	4/2/1950	6/1/1950	77000	05/02/1950		4/24/1950	7/3/1950	464706
1951	2/13/1951	6/11/1951	77000	02/28/1951	X	6/25/1951	8/7/1951	675636
1952	3/8/1952	7/18/1952	55600	04/26/1952		3/11/1952	6/4/1952	467978
1953	3/11/1953	4/24/1953	35000	04/08/1953		3/16/1953	5/25/1953	332818
1954	3/25/1954	5/20/1954	33200	04/25/1954	X	6/4/1954	7/14/1954	281277
1955	2/18/1955	4/11/1955	37400	02/26/1955		2/22/1955	3/14/1955	329887
1956	4/28/1956	6/11/1956	29500	06/02/1956		5/2/1956	5/6/1956	196612
1957	4/3/1957	8/12/1957	65500	05/06/1957		5/17/1957	8/5/1957	443031
1958	6/10/1958	8/26/1958	60200	06/22/1958		7/6/1958	8/24/1958	471904
1959	2/9/1959	6/11/1959	64000	02/19/1959	X	9/30/1959	10/21/1959	370894
1960	3/28/1960	7/22/1960	72800	04/07/1960		3/29/1960	7/18/1960	633884
1961	4/21/1961	5/30/1961	52800	05/16/1961		4/25/1961	6/17/1961	640777
1962	1/31/1962	6/4/1962	90500	03/29/1962		3/14/1962	5/23/1962	552651
1963	3/4/1963	4/13/1963	41000	03/09/1963		3/7/1963	4/12/1963	326552
1964	4/18/1964	5/17/1964	47800	04/29/1964	X	6/18/1964	7/5/1964	311830
1965	3/1/1965	5/31/1965	54400	04/18/1965		9/18/1965	10/17/1965	515170
1966	4/19/1966	6/26/1966	65400	05/26/1966		3/14/1966	6/8/1966	422269
1967	3/12/1967	6/7/1967	47600	04/11/1967	X	6/11/1967	7/20/1967	501239
1968	1/21/1968	3/8/1968	66500	02/11/1968	X	5/25/1968	6/14/1968	357149
1969	1/14/1969	3/1/1969	61900	02/09/1969	X	6/24/1969	8/4/1969	594761
1970	3/31/1970	7/15/1970	94000	05/22/1970		4/16/1970	7/3/1970	491968
1971	2/18/1971	4/15/1971	38500	03/02/1971		2/22/1971	5/21/1971	433502
1972	3/12/1972	6/4/1972	51000	05/01/1972		4/3/1972	5/30/1972	408511
1973	3/4/1973	7/20/1973	101000	05/02/1973		3/8/1973	6/27/1973	785220
1974	5/12/1974	7/28/1974	110000	06/29/1974		5/15/1974	7/13/1974	524087
1975	2/16/1975	6/17/1975	54700	03/03/1975		2/20/1975	6/13/1975	499423
1976	2/10/1976	4/22/1976	80300	03/13/1976		2/20/1976	6/10/1976	435967
1977	5/4/1977	5/22/1977	41600	05/13/1977	X	10/27/1977	11/26/1977	375225
1978	3/15/1978	6/17/1978	72400	05/20/1978		3/14/1978	6/12/1978	580797
1979	2/23/1979	6/8/1979	109000	04/19/1979		2/25/1979	6/8/1979	736195
1980	5/31/1980	6/29/1980	75700	06/07/1980	X	3/20/1980	5/4/1980	356344
1981	4/11/1981	9/21/1981	74500	05/24/1981		5/12/1981	6/11/1981	495649
1982	11/27/1982	1/31/1983	112000	12/12/1982		10/13/1982	1/23/1983	817301
1983	3/19/1983	6/27/1983	94600	04/19/1983		3/9/1983	6/13/1983	789024
1984	2/8/1984	7/2/1984	75700	03/28/1984		3/18/1984	7/20/1984	544476
1985	2/19/1985	5/10/1985	120000	03/10/1985		2/23/1985	5/9/1985	703017
1986	9/26/1986	11/17/1986	69600	10/11/1986		9/24/1986	11/17/1986	758017
1987	12/17/1987	12/31/1987	32600	12/30/1987	X	3/16/1987	5/15/1987	434819
1988	3/27/1988	5/4/1988	40100	04/14/1988	X	1/2/1988	1/8/1988	321193
1989	9/2/1989	9/30/1989	32800	09/18/1989		9/12/1989	9/21/1989	314919
1990	5/10/1990	8/12/1990	76500	06/27/1990		5/3/1990	8/14/1990	638072
1991	3/11/1991	6/24/1991	64200	05/31/1991		3/19/1991	7/7/1991	443880
1992	11/2/1992	12/31/1992	48500	11/25/1992		11/13/1992	12/31/1992	498346
1993	3/1/1993	6/3/1993	88000	04/23/1993	X	6/28/1993	10/18/1993	959925
1994	4/9/1994	5/24/1994	72900	04/22/1994		2/22/1994	6/1/1994	647549
1995	4/8/1995	7/14/1995	108000	05/31/1995		4/13/1995	7/18/1995	858170
1996	4/27/1996	7/15/1996	83100	06/07/1996		4/22/1996	7/16/1996	620293
1997	2/20/1997	5/3/1997	87500	03/06/1997		2/22/1997	6/11/1997	623827
1998	2/2/1998	6/9/1998	76000	05/16/1998		3/10/1998	5/19/1998	617849
1999	1/22/1999	4/2/1999	61500	02/04/1999	X	4/10/1999	7/23/1999	588383
2000	6/15/2000	7/28/2000	43000	07/01/2000		5/25/2000	7/30/2000	424512
2001	1/28/2001	4/9/2001	73300	03/04/2001		3/17/2001	7/15/2001	619080
2002	4/6/2002	7/8/2002	106000	05/20/2002		4/11/2002	7/8/2002	827701

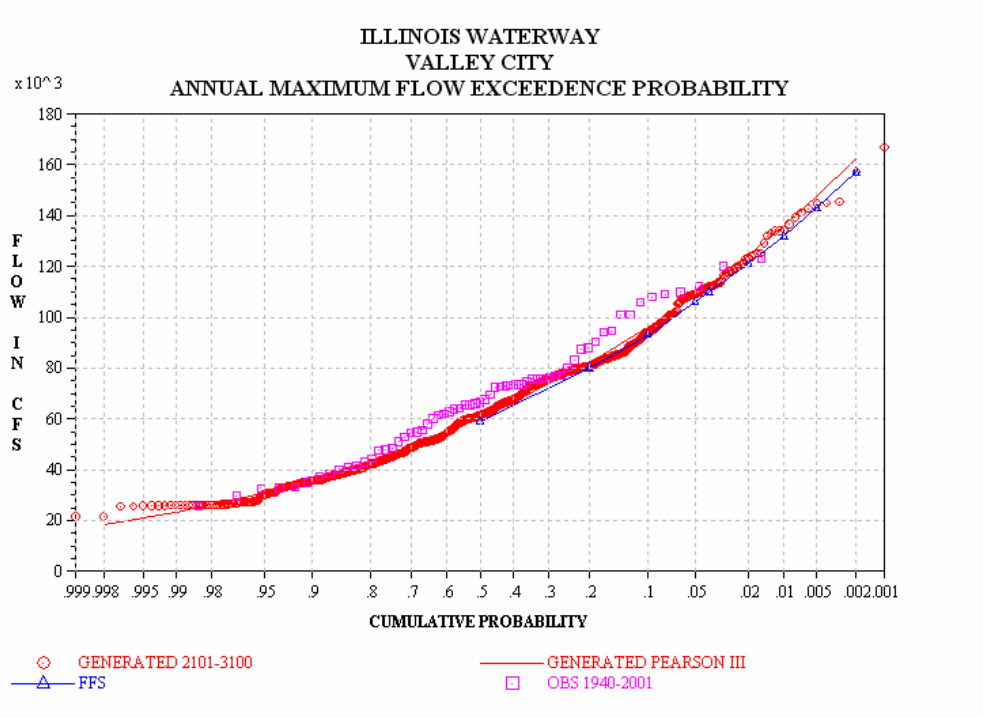

Figure 4.3. Maximum flow exceedence frequency of Valley City for FFS and for generated data from 2101 to 3100. The actual skew, -.193, is used for the generated Log-Pearson III curve. FFS applied a regional skew of -.2.

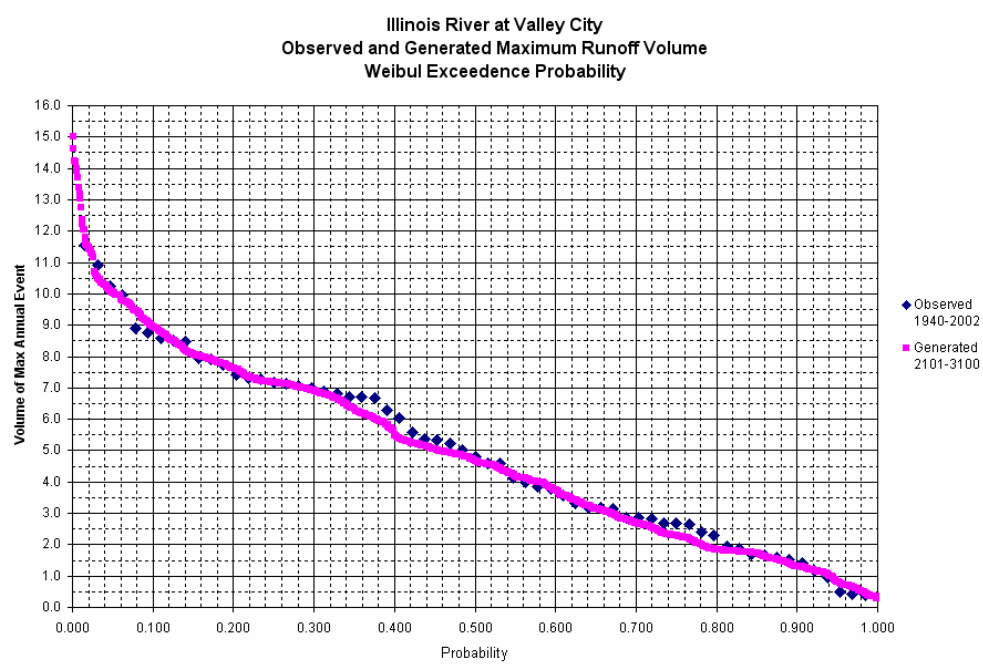

Figure 4.4. Event volume frequency at Valley City for observed data from 1940 to 2002 and for generated data from 2101 to 3100.

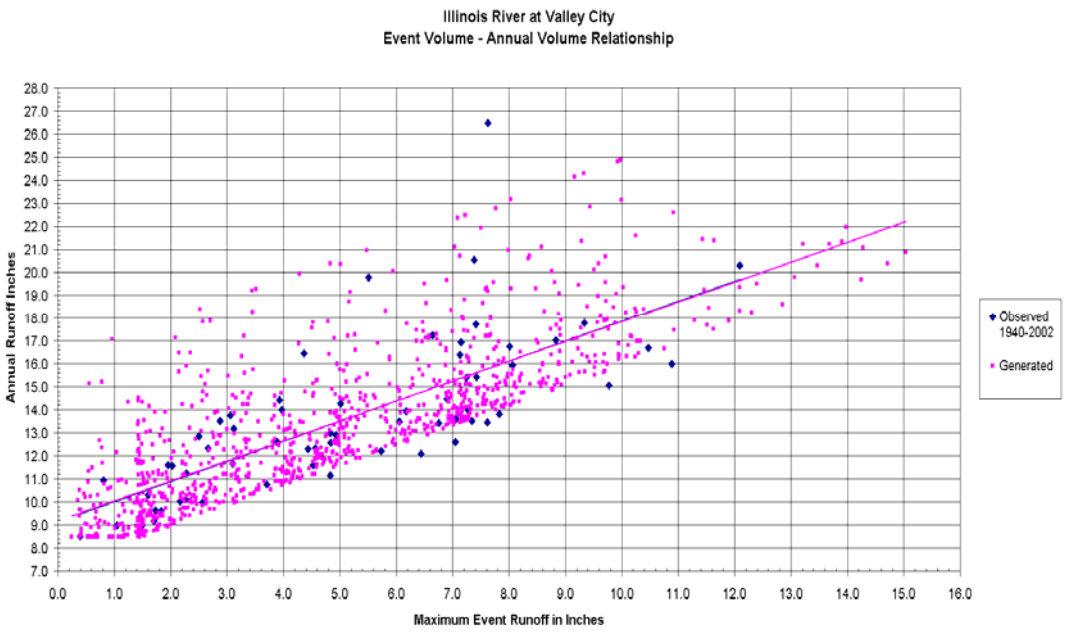

Figure 4.5. Generated and observed annual volume relationship.

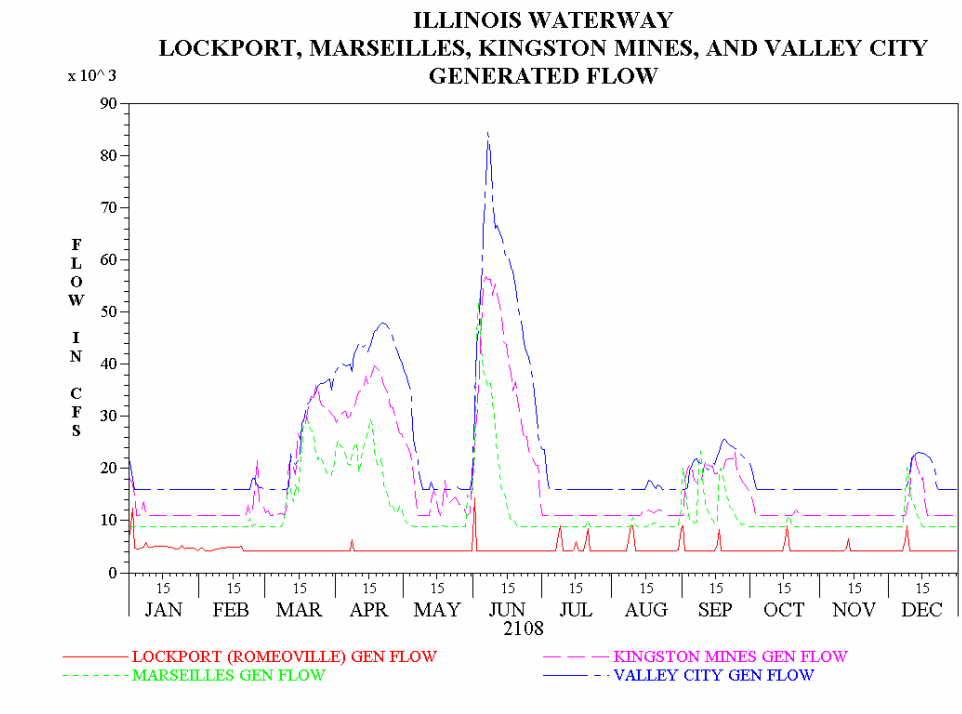

Figure 4.6. Generated flow hydrographs at Lockport, Marseilles, Kingston Mines, and Valley City for 2108. The April crest is coincident with the Mississippi River. The June crest is a headwater crest. The year 1980 is the pattern hydrograph.

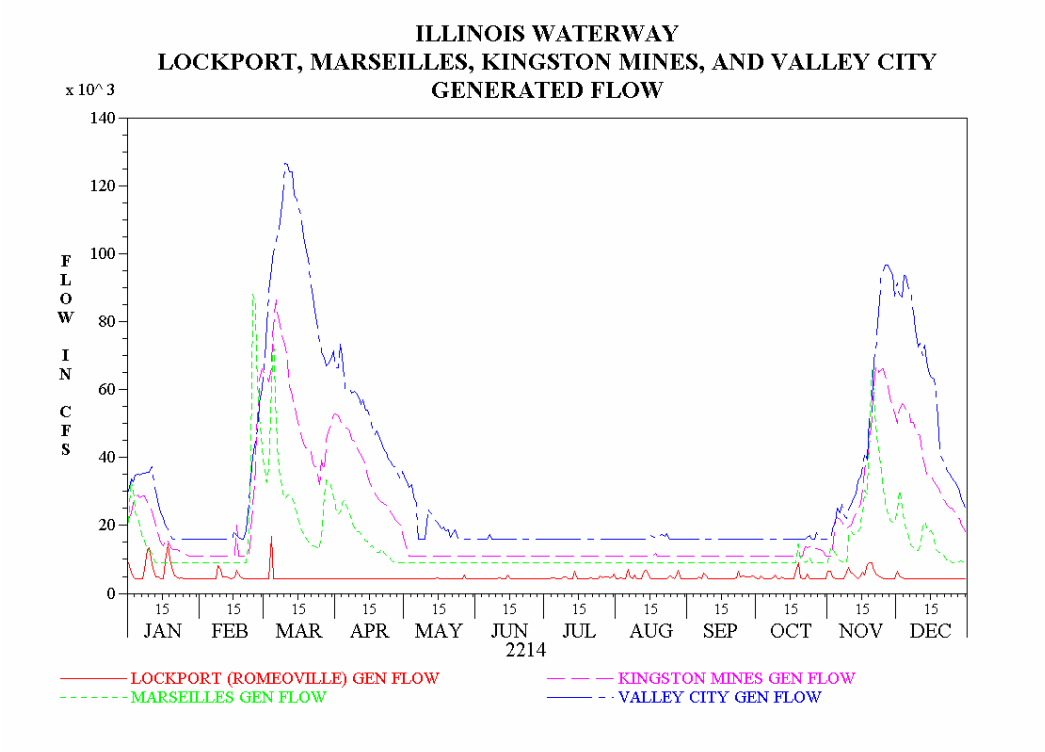

Figure 4.7. Generated flow hydrographs at Lockport, Marseilles, Kingston Miles, and Valley City for 2214. The March crest is coincident with the Mississippi River. Since the maximum Illinois River flow is coincident with the Mississippi, no secondary event is generated. The November crest is in the residual.

5.0 Generation of the Record at Clinton

5.1 The Origin of Floods

The flooding characteristics of the Mississippi Basin above Cairo result from two disparate processes. Snowmelt floods predominate above Davenport, Iowa and rainfall floods predominate downstream of Davenport. The rainfall flood can occur at any time of the year and snowmelt floods occur in the spring of the year. A rainfall flood may be atop a snowmelt flood. The height and volume of the snowmelt hydrograph builds as one moves downstream, but the basic shape of the hydrograph is maintained. In contrast, for large rivers, the rainfall event has multiple crests, corresponding to bursts of rainfall.

Table 5.1 compares top ten maximum floods at St. Paul, McGregor, Clinton and Keokuk. At Clinton nine of the top ten floods are from snowmelt. At Keokuk eight of the top ten floods are from rainfall. The transition from snowmelt to rainfall predominance occurs between Clinton and Keokuk. Figure 5.1 shows the flow hydrographs from the 1965 flood at St. Paul, McGregor, Clinton, Keokuk, Grafton, and St. Louis. The 1965 flood produced record stages above Davenport, but was not even the maximum event at Grafton and stations downstream. Figure 5.2 shows the hydrographs for year 2001. The snowmelt crest occurred in mid to late April. A burst of rainfall downstream of Clinton added a second crest in early May – three weeks after the snowmelt crest. This flood is an example of rainfall atop of a snowmelt event. Plots of other events are shown in the spreadsheet,

Table 5.1 Top Ten Mississippi River Floods Above Keokuk

St. Paul				McGregor				Clinton				Keokuk			
Year	Annual Maximum Flow CFS	Date	Flood Type	Year	Annual Maximum Flow CFS	Date	Flood Type	Year	Annual Maximum Flow CFS	Date	Flood Type	Year	Annual Maximum Flow CFS	Date	Flood Type
1965	171000	4/16/1965	S	1965	276000	4/24/1965	S	1965	307000	4/28/1965	S	1993	394,779	7/10/1993	R
1969	154000	4/15/1969	S	2001	247000	4/21/2001	S	2001	268000	4/23/2001	S	1973	322,909	4/24/1973	R
2001	142000	4/18/2001	S	1969	215000	4/22/1969	S	1993	238000	7/7/1993	R	2001	315,900	5/15/2001	R
1997	133000	4/12/1997	S	1997	200000	4/16/1997	S	1997	237000	4/19/1997	S	1965	294,943	5/1/1965	S
1952	124000	4/16/1952	S	1952	198000	4/22/1952	S	1969	231000	4/25/1969	S	1960	273,532	4/4/1960	R
1993	104000	6/26/1993	R	1993	187000	7/1/1993	R	1952	225000	4/26/1952	S	1986	254,055	10/6/1986	R
1951	92700	4/16/1951	S	1951	186000	4/22/1951	S	1951	222000	4/26/1951	S	1990	244,341	6/20/1990	R
1986	83000	5/6/1986	S	1975	183000	5/4/1975	S	1975	214000	5/7/1975	S	1974	243,739	5/22/1974	R
1957	78400	6/29/1957	R	1986	168000	4/11/1986	S	1973	207000	3/25/1973	S	1979	241,763	4/6/1979	R
1975	78100	5/4/1975	S	1954	166000	5/9/1954	S	1967	201000	4/14/1967	S	1975	239,630	5/9/1975	S

Rainfall floods were generated from Keokuk to Thebes. The exceptions were the floods generated from the 1965 pattern event, which was a snowmelt flood. Clinton and upstream gages are snowmelt dominated; therefore, transferring a rainfall flood from Keokuk to Clinton may be inconsistent; because, the snowmelt and rainfall events may not coincide.

We divide the floods into two groups -- floods where the annual maximum Keokuk flow is less than 110% of the annual maximum Clinton flow and all others. The former contains floods whose source is the upper basin (mainly snowmelt floods; although several floods are totally non-coincident) and latter contains mainly rainfall floods that are less dependent on the upper basin. Table 5.2 compares the source and coincidence of events at Clinton and Keokuk. From this table, we draw Figure 5.3, which compares flood crests at Clinton and Keokuk. The upper basin flood is a routing flood because the slope of the regression line approaches one; the flood crest originates upstream and increases only slightly as it moves downstream. The rainfall flood crest increases as tributaries contribute to its size.

For continuity, the pattern year for the generated years at Keokuk and Clinton must be the same; but the maximum events may be different. We optimize a relationship between Keokuk annual maximum flow and Clinton annual maximum rainfall and snowmelt flows. The optimized relationship reproduces the FFS flow frequency curve at Clinton. Figure 5.4 shows the optimized annual maximum flow transfer function between Keokuk and Clinton. Likewise we optimize event volume and annual volume transfer functions that reproduce observed statistics at Clinton. Figure 5.5 shows the optimized maximum event volume transfer function and Figure 5.6 shows the optimized annual volume transfer function between Keokuk and Clinton.

For example consider the generated year 2144. The maximum flow at Keokuk is 254,000 CFS. The pattern event is 1986. Because the crest at Keokuk is 40% greater than the crest at Clinton, this event is a rainfall event. From Figure 5.4 the crest at Clinton is 182,000 CFS. From Figure 5.5 and 5.6 the event volume and the annual volume would be 2.80” and 9.46” respectively. The starting and ending dates of the event are from Clinton, not Keokuk. Figure 5.7 shows the generated hydrographs for 2144 at Clinton and Keokuk.

As a second example consider the generated year 2874. The maximum flow at Keokuk is 303,000 CFS. The year 1965 is the pattern year. Because the crest Keokuk is 110% of the crest at Clinton, the 1965 event is a snowmelt event. From Figure 5.4, the crest at Clinton is 275,000 CFS. From Figure 5.5 and 5.6 the event volume and the annual volume would be 3.23” and 9.73” respectively. Figure 5.8 shows the generated hydrographs for 2874 at Clinton and Keokuk.

5.2 Statistics of Generated Hydrographs

The quality of the generated record is demonstrated by the comparing the statistics of the events to the statistics of the observed period. These statistics are completely summarized in Appendix C, but as an example, Figures 5.9 through 5.12 show the exceedence frequency, event volume frequency, annual volume frequency, and duration curves, respectively, at Clinton.

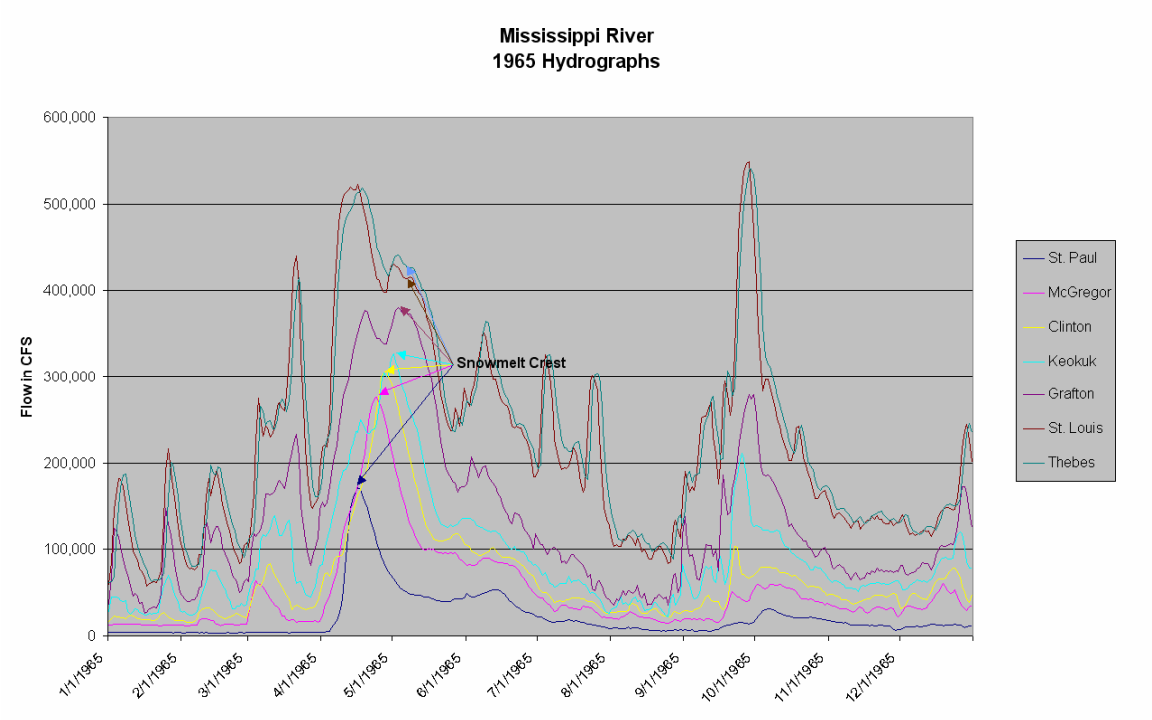

Figure 5.1. The 1965 snowmelt flood was the flood of record above Davenport, but the flood is lost in the rainfall bursts below Grafton. Even Keokuk, the light blue line, shows a rainfall burst in Mid-April prior to the snowmelt crest.

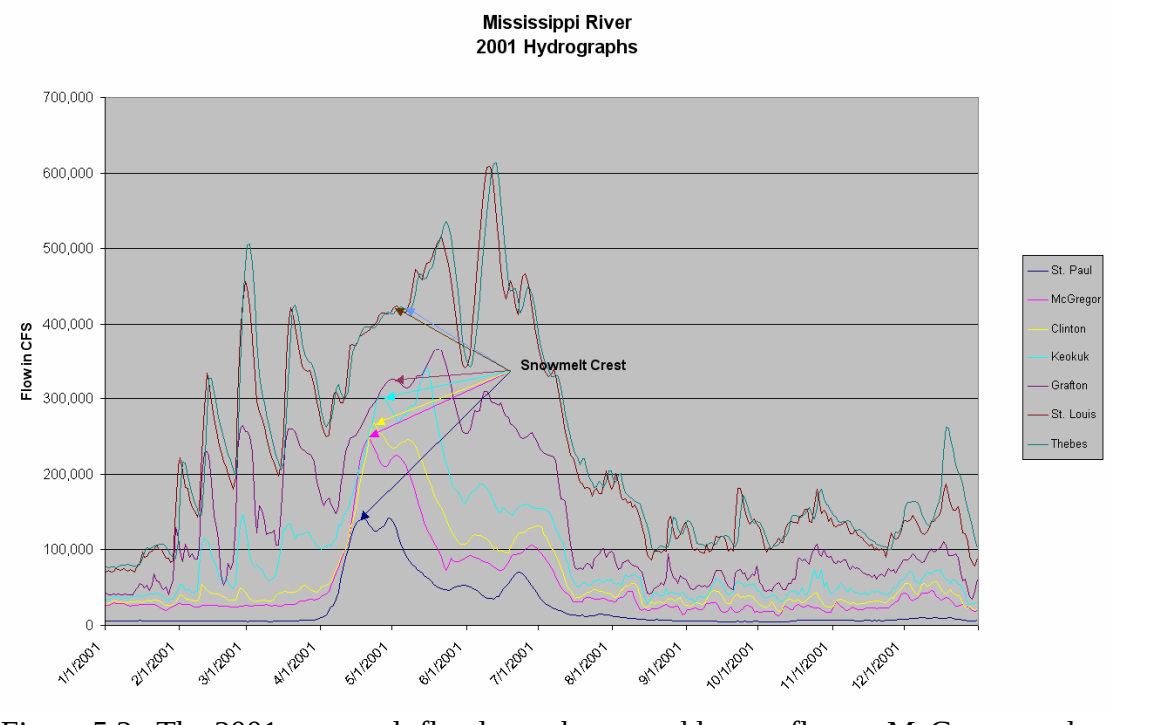

Figure 5.2. The 2001 snowmelt flood was the second largest flow at McGregor and Clinton, but the flood was lost in a burst of rainfall at Keokuk, which crested three weeks later.

Table 5.2 Mississippi River at Clinton and Keokuk											Routing	
Yearly Maximum Events at Clinton						Yearly Maximum Events at Keokuk Coincident with Thebes						
Year	Maximum Flow CFS (QC)	Date Maximum Flow	Snowmelt Flood	Runoff Inches	Annual Runoff Inches	Year	Maximum Flow CFS (QK)	Date Maximum Flow	Event Runoff Inches	Annual Runoff Volume Inches	Flood	QK < 1.1 *QC
1940	74100	6/19/1940		0.33	6.90	1940	60512	6/18/1940	0.14	6.36		L
1941	128000	4/23/1941	SN	1.85	8.93	1941	125984	11/8/1941	2.02	8.40		L
1942	170000	6/13/1942		2.52	9.10	1942	189580	6/16/1942	1.63	8.18	RO	
1943	159000	6/30/1943		2.76	9.72	1943	163341	4/19/1943	4.17	9.16		L
1944	168000	6/28/1944		4.66	9.30	1944	220032	5/28/1944	4.30	9.27		
1945	164000	3/31/1945	SN	2.88	9.42	1945	193456	3/27/1945	4.79	8.94		
1946	145000	3/28/1946	SN	2.14	8.61	1946	200530	1/12/1946	0.79	8.50		
1947	125500	6/15/1947		3.96	8.72	1947	215768	6/21/1947	4.87	9.18		
1948	108000	3/20/1948	SN	2.52	7.76	1948	213614	3/23/1948	3.24	7.83		
1949	85300	4/7/1949	SN	1.24	6.97	1949	140369	3/10/1949	2.21	7.00		
1950	130000	5/22/1950	SN	3.85	8.85	1950	167358	4/27/1950	2.12	8.47		
1951	222000	4/26/1951	SN	3.76	10.89	1951	177603	7/14/1951	1.65	10.75		L
1952	225000	4/26/1952	SN	3.43	9.92	1952	235276	4/29/1952	3.98	9.43	RO	L
1953	104000	4/5/1953	SN	3.11	9.21	1953	131553	4/2/1953	2.20	8.16		
1954	176000	5/14/1954	SN	2.41	8.72	1954	134802	7/2/1954	1.34	7.83		L
1955	96900	4/25/1955	SN	1.17	7.22	1955	105575	3/2/1955	0.52	6.94		L
1956	127000	4/20/1956	SN	1.80	7.29	1956	98418	4/28/1956	0.21	6.69		L
1957	103000	7/14/1957		1.45	7.08	1957	100507	7/16/1957	2.53	6.53	RO	L
1958	64500	4/15/1958	SN	0.60	6.50	1958	68681	7/16/1958	0.92	6.30		L
1959	112000	4/3/1959	SN	0.78	7.27	1959	89894	6/1/1959	0.80	7.48		L
1960	151000	5/18/1960	SN	3.52	8.72	1960	273532	4/5/1960	4.85	9.34		
1961	143000	4/2/1961	SN	1.67	7.63	1961	102767	4/29/1961	1.34	7.88		L
1962	138000	4/21/1962	SN	4.12	9.10	1962	211604	4/8/1962	3.28	9.00		
1963	90900	4/2/1963	SN	1.21	7.14	1963	120281	3/22/1963	1.12	6.81		
1964	84000	5/19/1964	SN	1.24	6.76	1964	63436	6/25/1964	0.34	6.46		L
1965	307000	4/28/1965	SN	5.30	11.23	1965	294943	5/2/1965	3.60	10.67	RO	L
1966	143000	4/1/1966	SN	3.37	8.72	1966	156615	4/3/1966	3.15	8.44	RO	L
1967	201000	4/14/1967	SN	2.65	8.65	1967	121708	6/23/1967	1.30	8.01		L
1968	128000	7/7/1968		1.87	8.61	1968	94293	5/30/1968	0.56	7.56		L
1969	231000	4/25/1969	SN	4.12	9.76	1969	198832	7/11/1969	1.81	9.85		L
1970	93000	6/8/1970		2.15	7.52	1970	135961	5/16/1970	2.38	7.73		
1971	168000	4/23/1971	SN	2.80	8.96	1971	173540	4/27/1971	3.45	8.53	RO	L
1972	153000	5/2/1972	SN	2.97	10.22	1972	180135	5/12/1972	2.50	9.94		
1973	207000	3/25/1973	SN	5.80	11.06	1973	322909	4/24/1973	6.85	12.39		
1974	158000	6/24/1974		3.84	8.72	1974	243739	5/22/1974	3.15	9.99		
1975	214000	5/7/1975	SN	2.94	9.33	1975	239630	5/10/1975	4.31	9.08	RO	
1976	154000	4/11/1976	SN	2.55	7.87	1976	199290	4/29/1976	3.59	7.78		
1977	57900	10/21/1977		0.63	6.48	1977	103584	11/3/1977	0.71	6.44		
1978	128000	4/21/1978	SN	1.64	8.66	1978	167585	4/24/1978	2.98	8.75		
1979	153000	5/5/1979	SN	5.66	10.62	1979	241763	4/6/1979	5.19	10.63		
1980	113000	10/1/1980		1.16	7.91	1980	124067	4/20/1980	1.42	7.86		L
1981	96800	4/14/1981	SN	1.39	7.81	1981	113296	5/15/1981	0.74	7.85		
1982	163000	4/29/1982	SN	4.11	10.15	1982	170759	12/5/1982	3.31	11.11		L
1983	179000	3/18/1983	SN	4.55	10.66	1983	210620	3/22/1983	4.92	11.06	RO	
1984	134000	5/11/1984	SN	2.84	10.52	1984	180795	5/12/1984	3.60	10.76		
1985	139000	4/8/1985	SN	3.53	10.06	1985	197809	3/6/1985	3.36	9.73		
1986	201000	10/6/1986		2.52	12.85	1986	254055	10/5/1986	2.91	12.68		
1987	66000	4/3/1987	SN	1.24	6.75	1987	88751	4/3/1987	1.40	6.68		
1988	65800	4/6/1988	SN	1.17	6.56	1988	99983	4/5/1988	0.92	6.60		
1989	104000	4/6/1989	SN	1.50	6.98	1989	70592	9/11/1989	0.23	6.64		L
1990	123000	6/24/1990		1.49	8.33	1990	244341	6/21/1990	3.66	8.77		
1991	137000	6/11/1991		4.67	10.72	1991	176907	4/21/1991	5.02	10.30		
1992	147000	4/30/1992	SN	3.26	9.62	1992	152837	11/25/1992	1.51	9.36		L
1993	238000	7/7/1993		10.26	14.80	1993	394779	7/10/1993	7.74	17.22		
1994	147000	5/7/1994	SN	3.75	9.77	1994	146718	5/10/1994	3.41	8.68	RO	L
1995	120000	4/30/1995	SN	3.98	10.18	1995	192932	5/14/1995	3.97	9.65		
1996	186000	5/1/1996	SN	5.31	10.16	1996	218635	5/13/1996	4.07	9.58		
1997	237000	4/19/1997	SN	3.79	10.33	1997	233626	4/22/1997	4.72	9.55	RO	L
1998	178000	4/11/1998	SN	2.19	9.39	1998	235174	4/15/1998	3.25	10.19		
1999	144000	5/19/1999	SN	5.28	9.64	1999	193860	5/28/1999	4.63	9.77		
2000	125000	6/15/2000		2.50	8.10	2000	194330	6/18/2000	2.82	8.13		
2001	268000	4/23/2001	SN	6.39	11.36	2001	315900	5/15/2001	6.66	11.05		
2002	166000	4/25/2002	SN	2.40	9.85	2002	183685	6/9/2002	3.64	8.82		

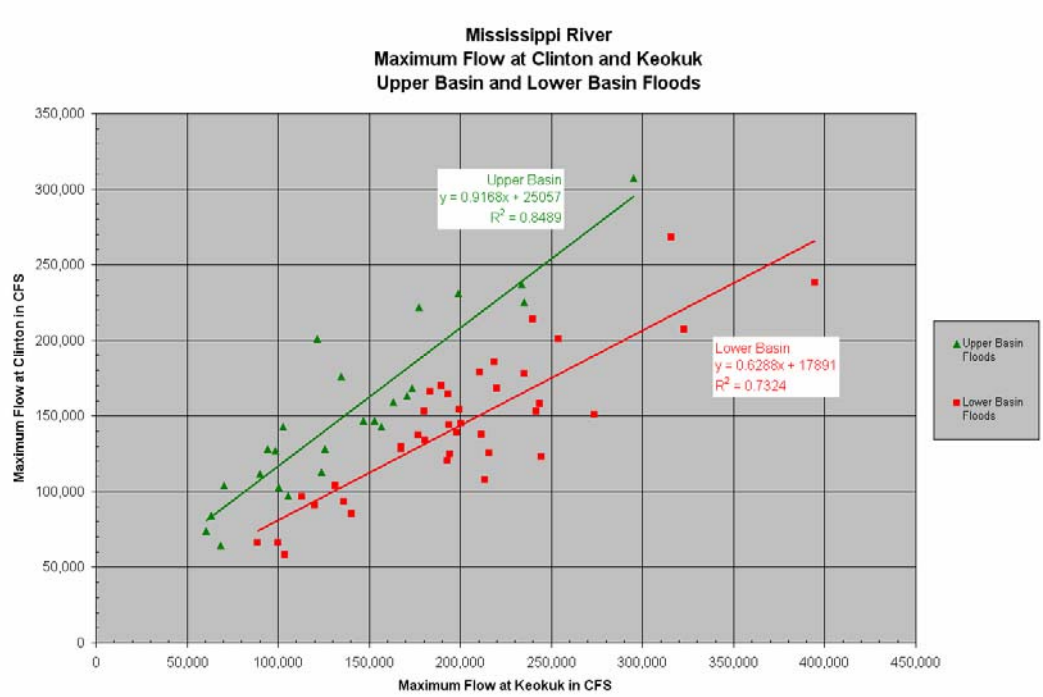

Figure 5.3. Upper basin flood and lower basin floods. Upper basin floods originate above Clinton and they are primarily from melting snowpack. Between Clinton and Keokuk, upper basin floods are routed through the river with only a small increase in the crest; hence the slope of the regression line approaches one. In contrast the crest of rainfall floods increase markedly as the swollen tributaries contribute to the flow of the main stem.

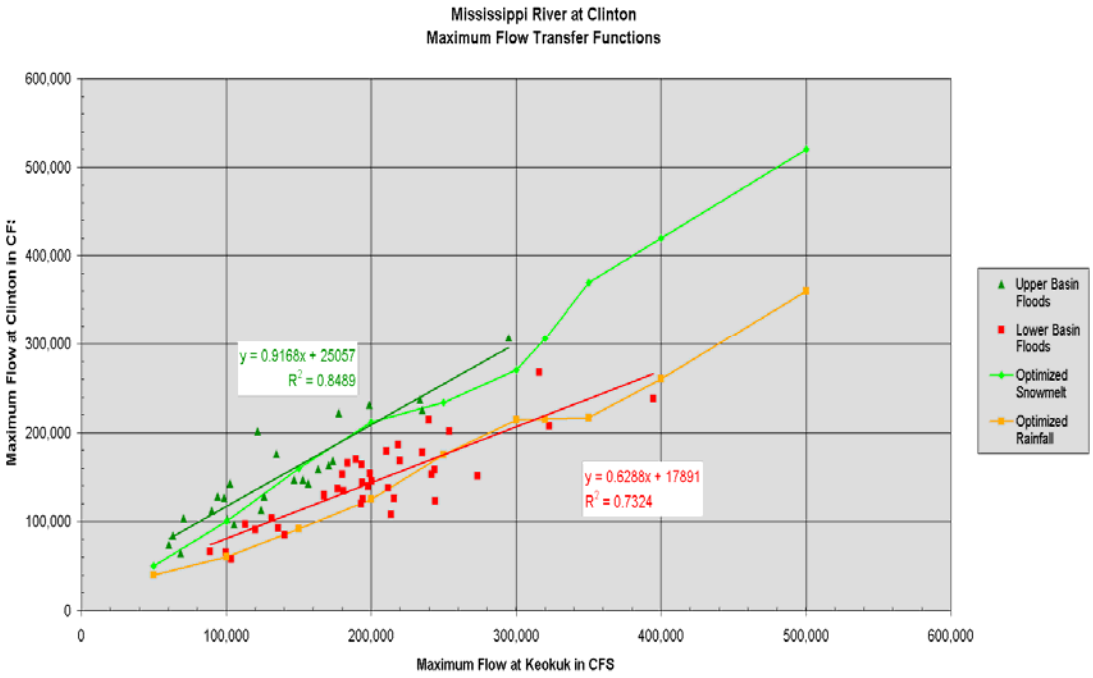

Figure 5.4. Optimized upper basin (mainly snowmelt) and lower basin (rainfall) maximum flow transfer functions. The optimized functions reproduce the FFS frequency relationships.

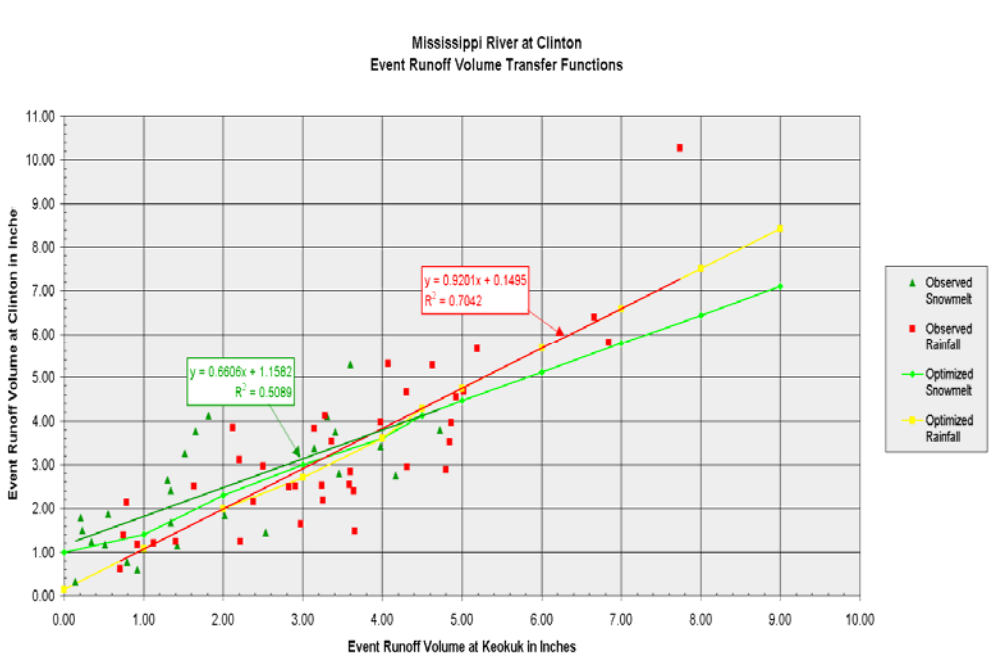

Figure 5.5. Optimized upper basin and lower basin event volume transfer functions. The optimized functions reproduce the observed event volume frequency relationships.

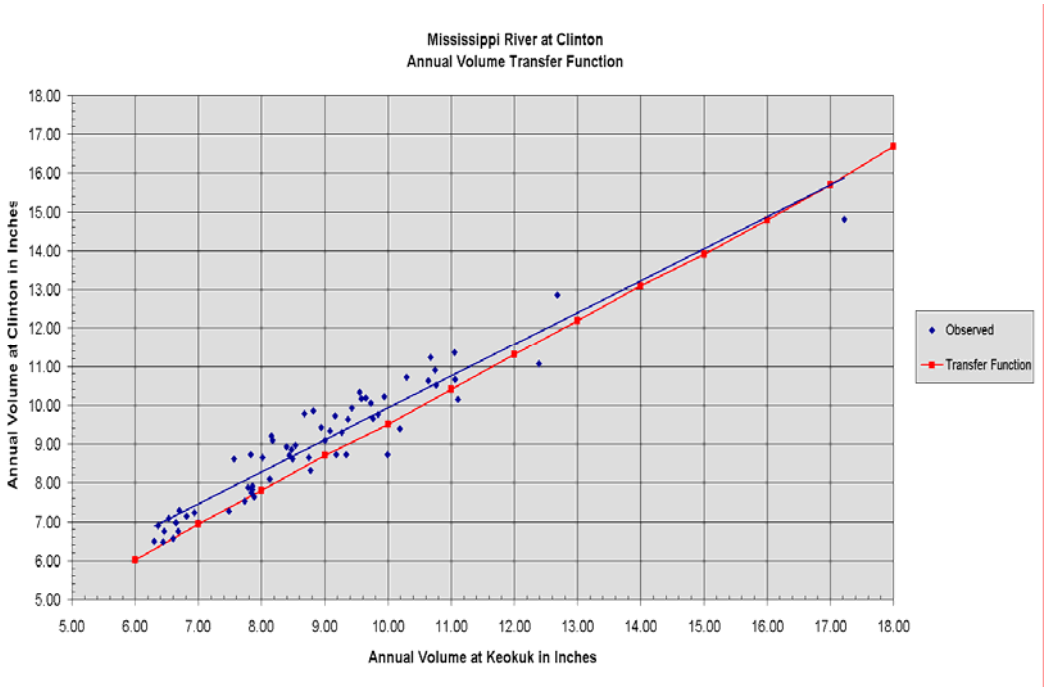

Figure 5.6. Optimized annual volume transfer function.

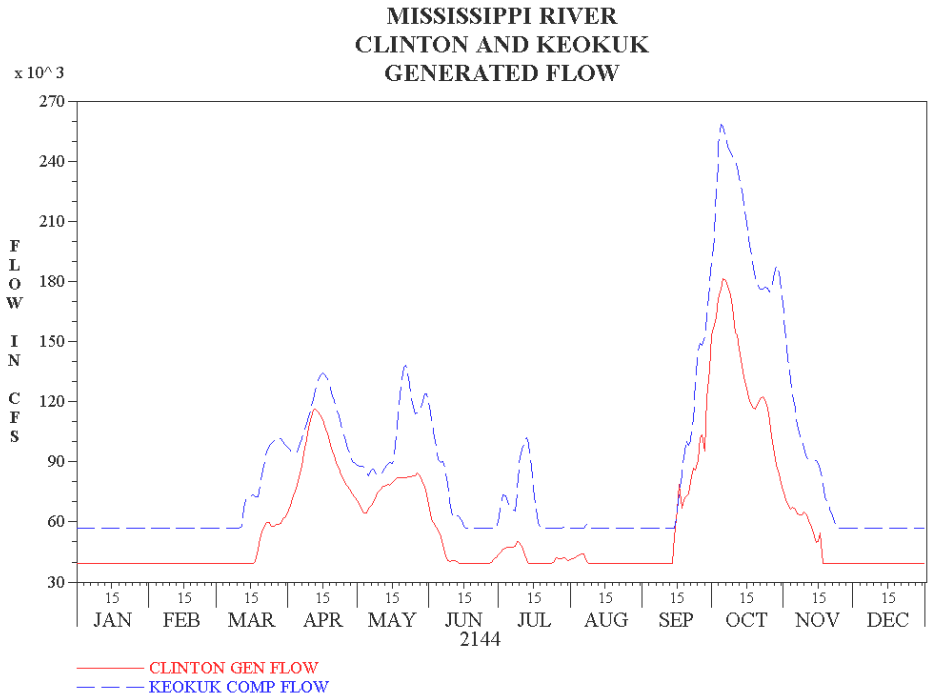

Figure 5.7 Generated hydrographs at Clinton and Keokuk. The pattern event was the 1986 flood, a rainfall event in early October.

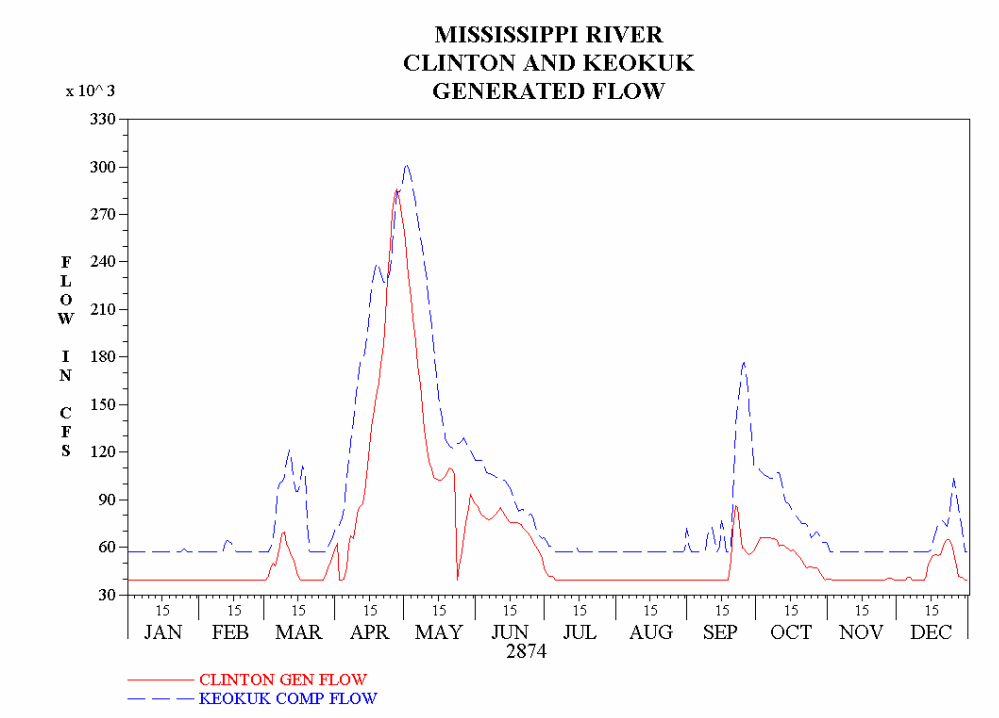

Figure 5.8. Generated hydrographs at Clinton and Keokuk for 2874. The pattern event was the 1965 flood, a snowmelt event.

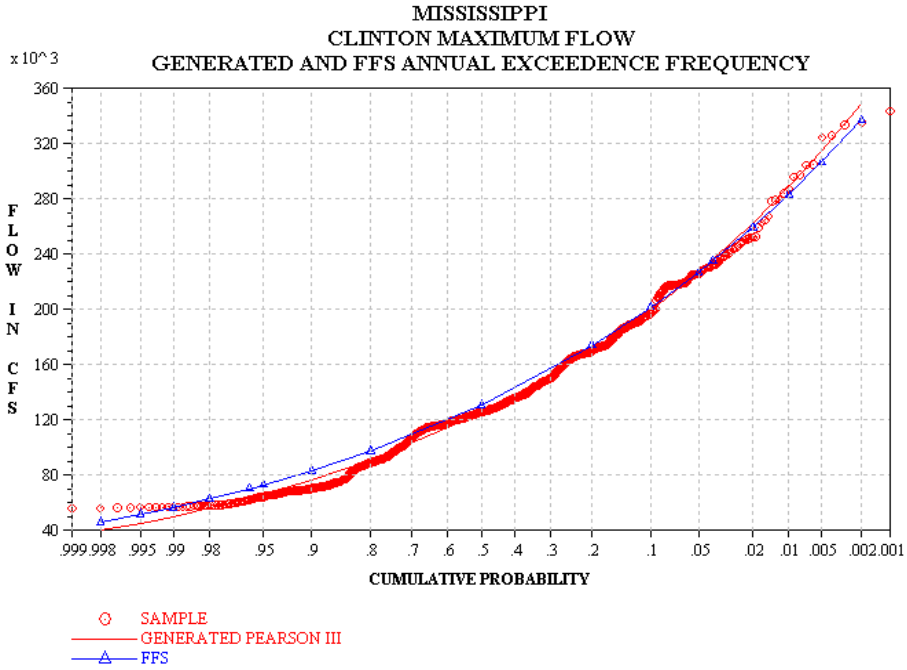

Figure 5.9 Maximum flow exceedence frequency at Clinton for FFS and for generated data from 2101 to 3100. The actual skew, -0.114, is used for the generated Log-Pearson III curve. FFS applied a regional skew of –0.100.

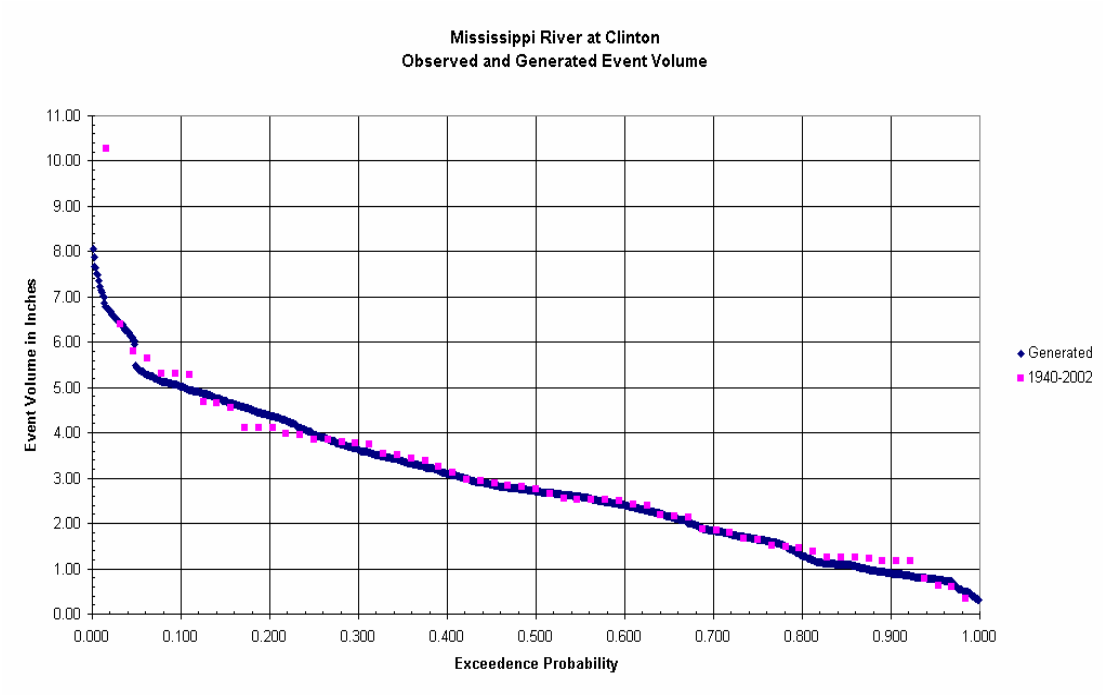

Figure 5.10. Event volume frequency at Clinton for observed data from 1940 to 2002 and for generated data from 2101 to 3100.

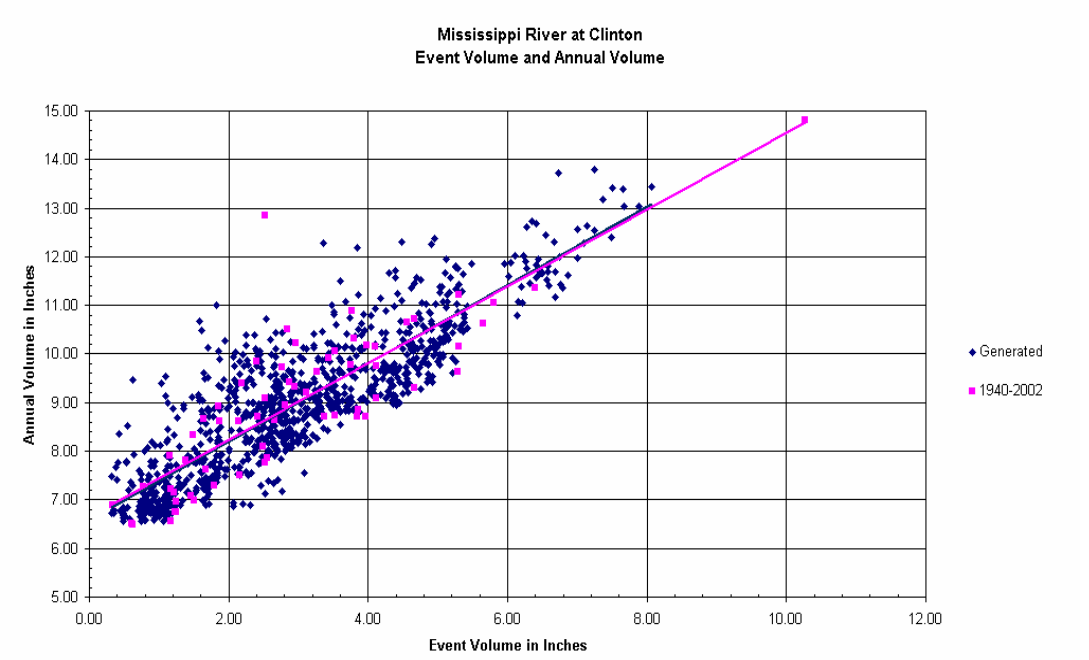

Figure 5.11. Annual volume at Clinton for observed data from 1940 to 2002 and for generated data from 2101 to 3100.

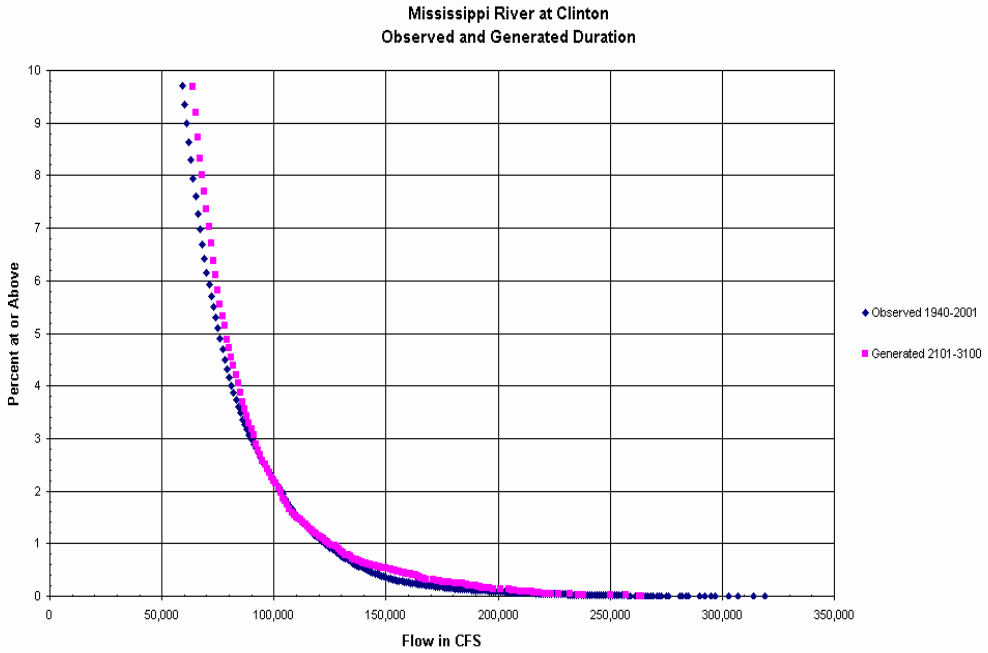

Figure 5.12. Annual duration at Clinton below the 10% level for observed data from 1940 to 2002 and for generated data from 2101 to 3100.

6.0 Generation of the Record at McGregor, Winona, St. Paul, and Anoka

6.1 FFS and Observed Data

For McGregor, Winona, and St. Paul (Anoka was not a part of the FFS study), the Weibul scatter of the observed annual maximum flow plotted above the official FFS frequency curve. Figure 6.1 demonstrates this disparity at McGregor. This difference was a problem when generating data, since the generated data is closely tied to the observed time series.

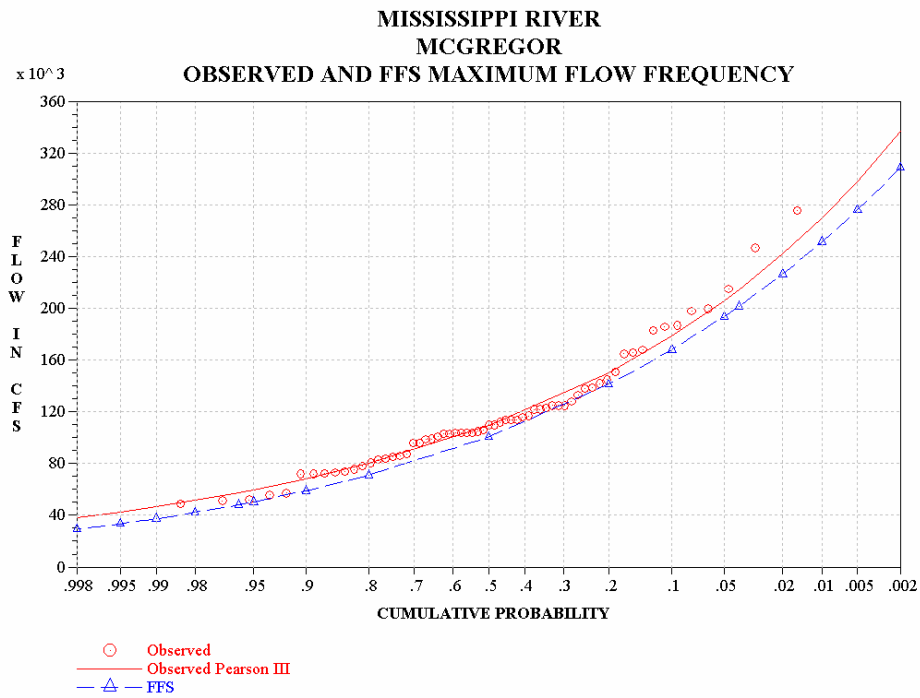

Figure 6.1. Weibul scatter plot of observed data compared to the official FFS frequency curve at McGregor. Despite the observed data, the generated data was adjusted to reproduce the FFS frequency curve.

FFS statistics were assumed correct; therefore, the observed flow data was adjusted downward to reproduce the FFS statistics. We assumed that the shape of the hydrographs was correct, but the flow record was wrong. Therefore, from Figure 6.1, a flow of 167,000 CFS was actually 164,000 CFS. Relative corrections from Figure 6.1 were applied across the board to entire flow record.

6.2 Generated Data at McGregor, Winona, St. Paul, and Anoka

Appendix D compares the generated and FFS statistics at McGregor, Winona, St. Paul, and Anoka. As an example, Figures 6.2 through 6.5 compare the statistics at McGregor. Figure 6.6 compares the generated hydrographs at Anoka, St. Paul, Winona, and McGregor for the year 2412. That year uses 1993 as its pattern hydrograph. Figure 6.7 shows

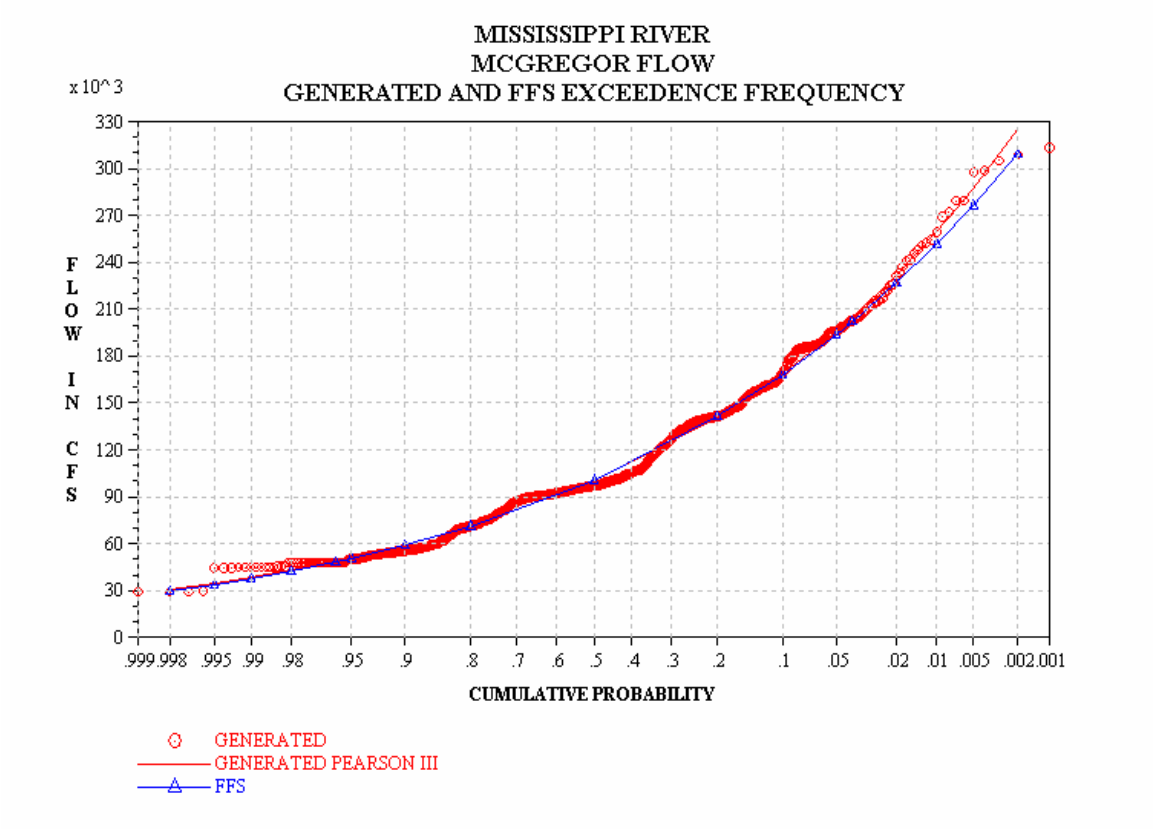

Figure 6.2. Generated and FFS statistics at McGregor.

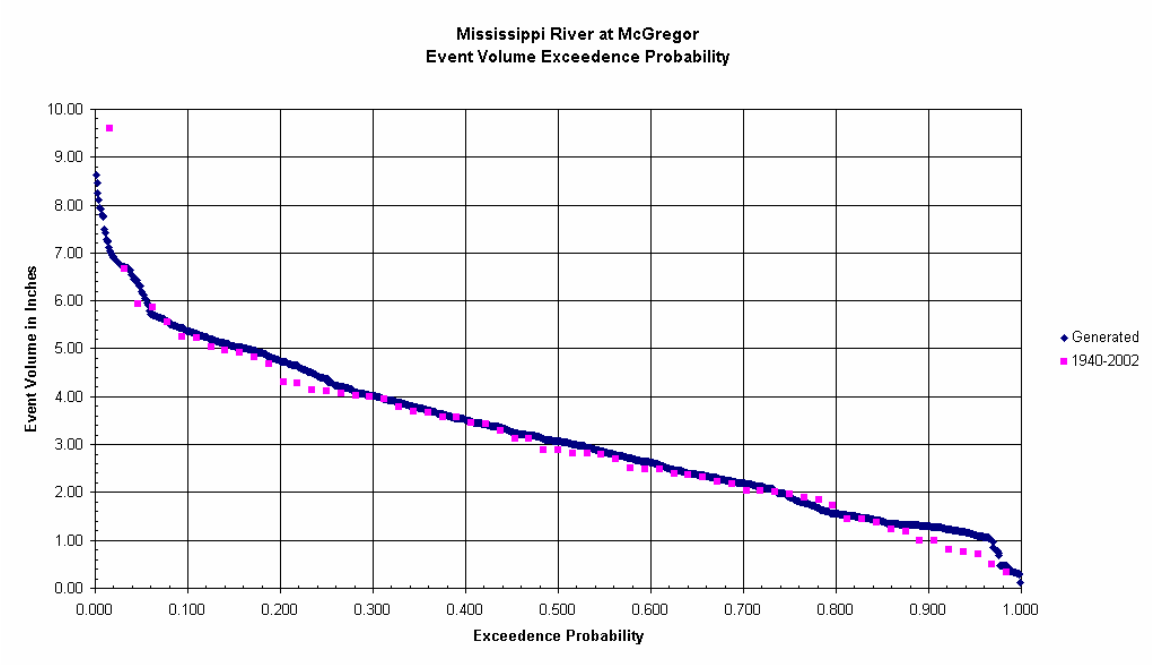

Figure 6.3. Generated and observed event volume frequency at McGregor.

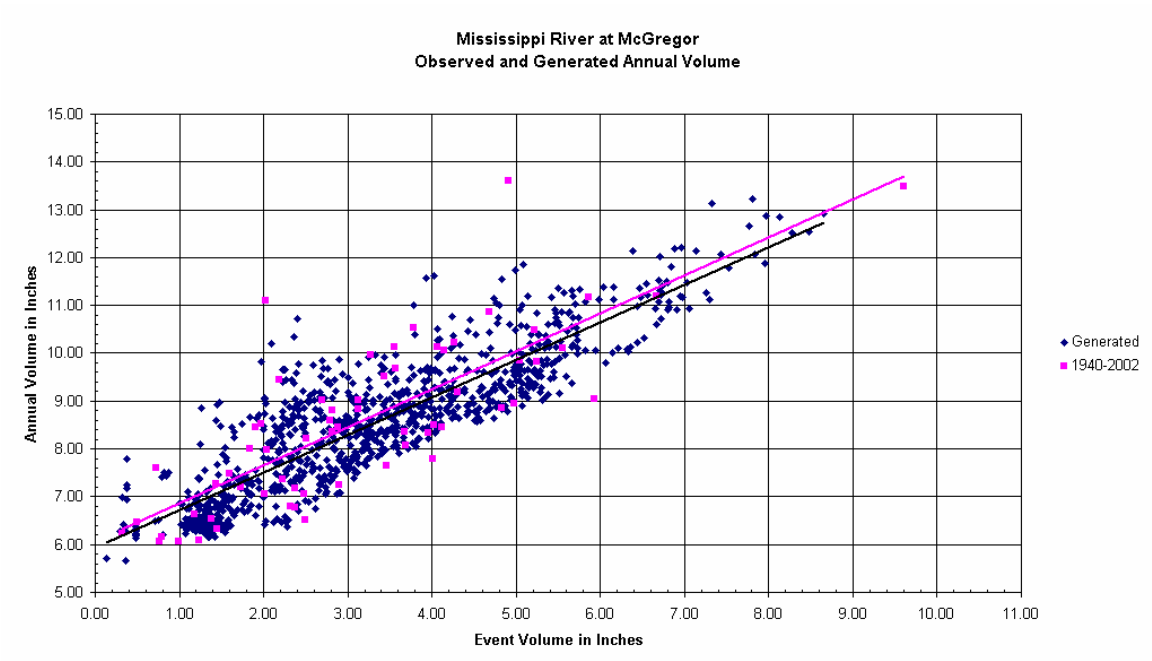

Figure 6.4. Generated and observed annual volume at McGregor.

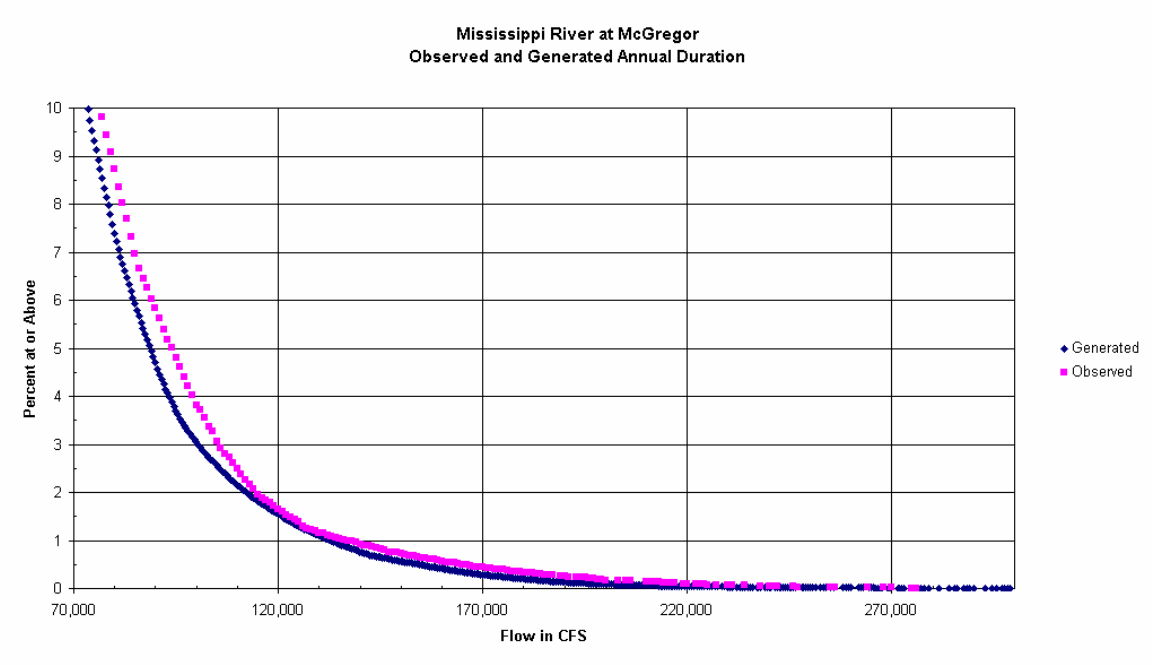

Figure 6.5. Generated and observed duration below the 10% level at McGregor.

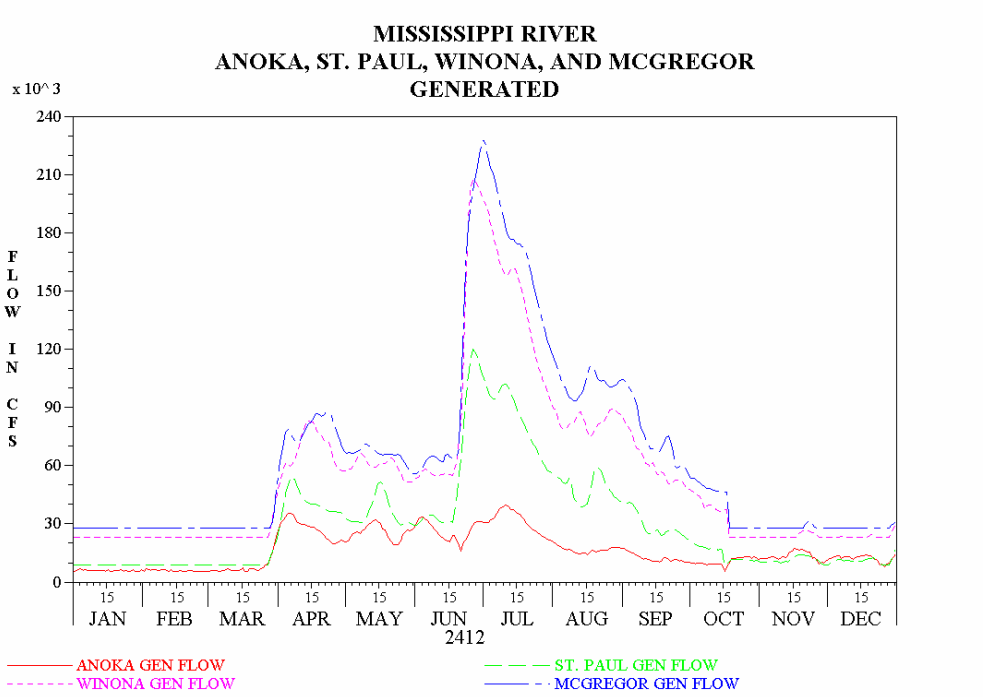

Figure 6.6. Generated hydrographs at Anoka, St. Paul, Winona, and McGregor. The year 2412 uses 1993 as its pattern year.

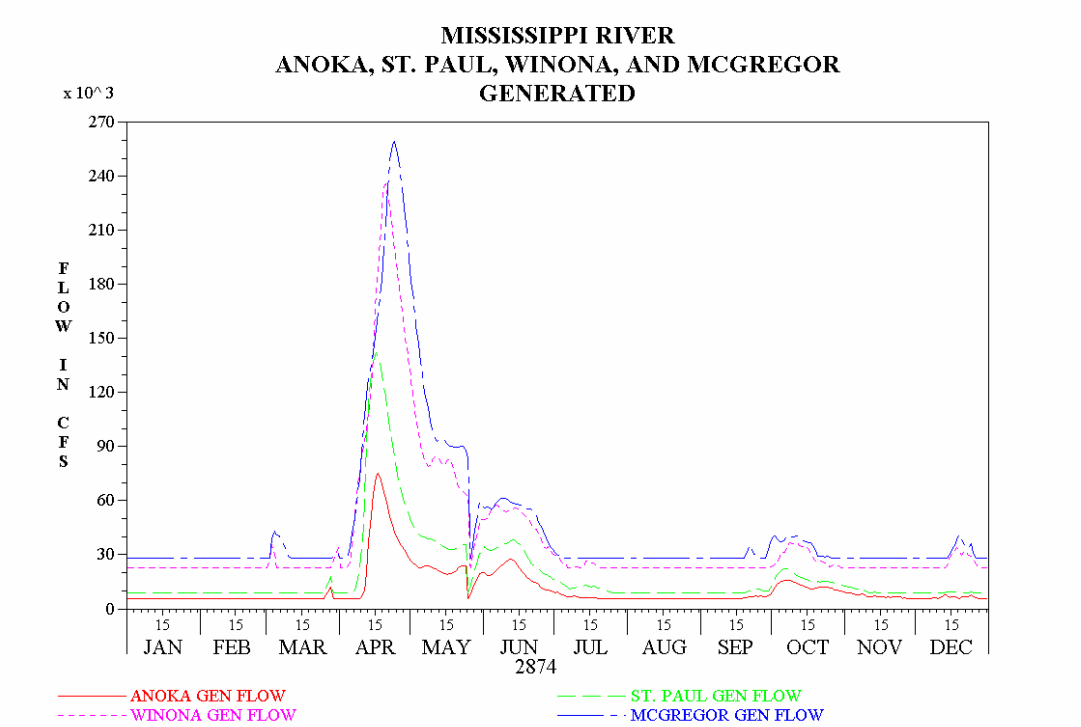

Figure 6.7. Generated hydrographs for 2874. That year uses 1965 as its pattern year.

7.0 Ungaged Inflow

We have estimated period of generated data (POGD) hydrographs at the primary mainstem gaging stations and at all of downstream tributary gaging stations. Still, there is a sizable area of ungaged drainage between each gaging station. Ungaged inflow has been estimated for FFS using the "Null Interior Boundary Condition" from the UNET program; likewise the "Null Interior Boundary Condition" was used to estimate ungaged inflow for the POGD. This algorithm produces ungaged inflow that produces a perfect reproduction of the flow at the target gages. We divide the optimization into four regions:

1) Keokuk to Thebes.

    a) Keokuk to Lock and Dam 24.
    b) Lock and Dam 24 and Valley City to St. Louis.
    c) St. Louis to Chester.
    d) Chester to Thebes.

2) McGregor to Keokuk.

    a) McGregor to Clinton.
    b) Clinton to Keokuk.

3) Anoka to McGregor.

    a) Anoka to St. Paul.
    b) St. Paul to Winona.
    c) Winona to McGregor.

4) Illinois River, Lockport to Valley City.

    a) Lockport to Marseilles.
    b) Marseilles to Kingston Mines.
    c) Kingston Mines to Valley City.

The ungaged inflow optimizations are arduous calculations. Each region required about 150 hours of computer time.

8.0 Conclusions and Recommendations.

So the algorithm obviously works. The algorithm works beyond expectations from Keokuk to Thebes and from Anoka to Clinton. The transfer function, which simulates rainfall and snowmelt events, (Figures 5.3 to 5.6) from Keokuk to Clinton is acceptable but does need improvement. The algorithm works well between Lockport and Valley City, but the algorithm that produces non-coincident events (Figures 4.1 and 4.2) needs more study. The coincidence between the Illinois and Mississippi Rivers is nearly perfect and the non-coincident events could have been ignored, but what about rivers, which are nearly independent, where coincidence is happenstance? The algorithm requires further study to prove its applicability.

Lastly I have developed a better procedure than the "Null Internal Boundary Condition" for optimizing ungaged inflow. I have developed an extremely accurate procedure for determining ungaged inflow.